https://doi.org/10.5194/egusphere-2023-1283
Preprint. Discussion started: 14 June 2023


# Sensitivities of cloud radiative effects to large-scale meteorology and aerosols from global observations

Hendrik Andersen[1,2], Jan Cermak[1,2], Alyson Douglas[3], Timothy A. Myers[4,5], Peer Nowack[6], Philip Stier[3], Casey J. Wall[7], and Sarah Wilson Kemsley[8]

[1]Institute of Meteorology and Climate Research, Karlsruhe Institute of Technology (KIT), Karlsruhe, Germany
[2]Institute of Photogrammetry and Remote Sensing, Karlsruhe Institute of Technology (KIT), Karlsruhe, Germany
[3]Atmospheric, Oceanic and Planetary Physics, Department of Physics, University of Oxford, UK
[4]Cooperative Institute for Research in Environmental Sciences (CIRES), University of Colorado, Boulder, USA
[5]Physical Science Laboratory, National Oceanic and Atmospheric Administration, Boulder, USA
[6]Institute of Theoretical Informatics, Karlsruhe Institute of Technology (KIT), Karlsruhe, Germany
[7]Department of Geosciences, University of Oslo, Oslo, Norway
[8]Climatic Research Unit, School of Environmental Sciences, University of East Anglia, Norwich, UK

**Correspondence:** Hendrik Andersen (hendrik.andersen@kit.edu)

**Abstract.** The radiative effects of clouds make a large contribution to the Earth's energy balance, and changes in clouds constitute the dominant source of uncertainty in the global warming response to carbon dioxide forcing. To characterize and constrain this uncertainty, cloud controlling factor (CCF) analyses have been suggested that estimate sensitivities of clouds to large-scale environmental changes, typically in cloud-regime specific multiple linear regression frameworks. Here, local sensitivities of cloud radiative effects to a large number of controlling factors are estimated in a regime-independent framework from 20 years of near-global satellite observations and reanalysis data using statistical learning. A regularized linear regression (ridge regression) is shown to skillfully predict anomalies of shortwave ($R^2$ = 0.63) and longwave CRE ($R^2$ = 0.72) in independent test data on the basis of 28 CCFs, including aerosol proxies. The sensitivity of CRE to selected CCFs is quantified and analyzed. CRE sensitivities to sea-surface temperature and estimated inversion strength are particularly pronounced in low-cloud regions and generally in agreement with previous studies. The analysis of CRE sensitivities to three-dimensional wind field anomalies reflects that CREs in tropical ascent regions are mainly driven by variability of large-scale vertical velocity in the upper troposphere. In the subtropics, CRE is sensitive to free-tropospheric zonal and meridional wind anomalies, which are likely to encapsulate information on synoptic variability that influences subtropical cloud systems by modifying wind shear and thus turbulence and dry-air entrainment in stratocumulus clouds, as well as variability related to midlatitude cyclones. Different proxies for aerosols are analyzed as CCFs, with satellite-derived aerosol proxies showing a larger CRE sensitivity than a proxy from an aerosol reanalysis, likely pointing to satellite aerosol retrieval biases close to clouds leading to overestimated aerosol sensitivities. Sensitivities of shortwave CRE to all aerosol proxies indicate a pronounced cooling effect from aerosols in stratocumulus regions that is counteracted to a varying degree by a longwave warming effect. The analysis may guide the selection of CCFs in future sensitivity analyses aimed at constraining cloud feedback and climate forcings from aerosol-cloud interactions, using both data from observations and global climate models.

https://doi.org/10.5194/egusphere-2023-1283
Preprint. Discussion started: 14 June 2023


## 1 Introduction

Clouds are main modulators of the Earth's energy budget, cooling the Earth by about 20 W m$^{-2}$ on average. This cooling is driven by clouds reflecting incoming shortwave solar radiation, therefore reducing the energy uptake of the Earth system by about 47 W m$^{-2}$. Clouds increase the Earth atmosphere's opacity in the infrared, however, absorbing longwave radiation emitted by the warmer Earth surface, and emitting less longwave radiation themselves due to the lower cloud-top temperatures. The combined effect of longwave absorption and emission leads to a warming of around 28 W m$^{-2}$ (numbers from Forster et al. (2021)). These effects of clouds on the Earth's energy budget are called cloud radiative effects (CRE), and are defined as the difference in radiation between "all-sky" (cloudy and clear-sky) and (hypothetical) "clear-sky" conditions (Ramanathan et al., 1989). While shortwave CRE (CRE$_{SW}$) are mainly related to cloud fraction and microphysics (number concentration of water/ice particles and the amount of liquid water/ice), longwave CRE (CRE$_{LW}$) are mainly driven by cloud altitude and thus cloud-top temperature, but also cloud fraction (Voigt et al., 2021). As such, any changes to cloud patterns, be it occurrence, microphysics or macrostructure have important implications for the Earth's energy balance. In a changing climate, clouds may be altered due to changes in the large-scale environment (cloud feedbacks) or due to a change in aerosol concentration (aerosol-cloud interactions, both are discussed below). In spite of their importance for the Earth's climate system, considerable uncertainty exists as to how clouds may respond to changes in their environmental controls, ultimately impeding the quantification of climate sensitivity, i.e. the global temperature increase following a doubling of the carbon dioxide ($CO_2$) concentration in the atmosphere compared to preindustrial levels (Zelinka et al., 2020; Forster et al., 2021).

Cloud feedbacks describe how clouds respond to and feedback on climate warming and are a major uncertainty in climate science. Many cloud feedbacks have been described in the literature, which relate changes in cloud altitude, phase, albedo, or coverage with global warming, typically in cloud-regime specific frameworks (i.e., very few CCFs targeting a specific cloud type, e.g. Zelinka et al., 2016; Mülmenstädt et al., 2021; Murray et al., 2021; Zelinka et al., 2022). The most extensively studied cloud feedback is the (positive) low-cloud feedback (e.g. Klein et al., 2017; Scott et al., 2020; Myers et al., 2021; Cesana and Del Genio, 2021), which has been shown to be a main cause for the variation in climate sensitivity estimates in global climate models (Bony and Dufresne, 2005; Zelinka et al., 2020). Global satellite observations can help reduce this uncertainty by constraining cloud feedbacks with observation-based sensitivity estimates of clouds (and their radiative effects) to changes in their large-scale environmental controls (cloud controlling factors, CCFs). This is traditionally done in regime-specific cloud-controlling factor analyses, where cloud anomalies are regressed upon a small number of local CCF anomalies using a ordinary least squares regression (OLS). Recently, a statistical learning framework (ridge regression), which allows for robust sensitivity estimation with many co-linear CCFs, have been used to predict cloudiness and constrain their feedbacks by not only using local CCF anomalies, but also their large-scale patterns (Andersen et al., 2020; Ceppi and Nowack, 2021). While regime-specific CCF frameworks are relatively well understood and thought to include the most relevant large-scale

https://doi.org/10.5194/egusphere-2023-1283
Preprint. Discussion started: 14 June 2023


environmental controls of clouds in specific regimes (e.g. Klein et al., 2017), they do not necessarily include all relevant CCFs that may change in a warmer climate and thus influence the estimation of cloud feedbacks.

Atmospheric aerosols are another important driver of variability and trends in CRE (Quaas et al., 2022), because aerosols, by acting as cloud condensation nuclei (CCN), are drivers of cloud droplet number concentration in liquid water clouds. Under the assumption of a constant liquid water path, this leads to smaller cloud droplets, and an increase in cloud reflectivity (Twomey, 1977). These instantaneous changes in cloud droplet characteristics may lead to the suppression or delay of precipitation, which in turn may trigger subsequent adjustments of the cloud field, such as an increase in cloud fraction or liquid water path (Albrecht, 1989), further altering CRE. Observational and modeling studies on the cloud fraction adjustment mostly find positive relationships (Kaufman and Koren, 2006; Gryspeerdt et al., 2016; Andersen et al., 2017; Christensen et al., 2020; Chen et al., 2022), while the sign of the liquid water path adjustment is still debated (Ackerman et al., 2004; Malavelle et al., 2017; Gryspeerdt et al., 2019; Rosenfeld et al., 2019; Toll et al., 2019; Manshausen et al., 2022; Zipfel et al., 2022; Wall et al., 2022). In convective cloud systems, a deepening or invigoration has been suggested, however, this effect is still elusive (Koren et al., 2005, 2010, 2014; Altaratz et al., 2014; Sarangi et al., 2018; Marinescu et al., 2021). Depending on the ambient air temperature, aerosols can also act as ice nucleating particles, potentially increasing ice crystal number concentration, and leading to further cloud adjustments (Hoose and Möhler, 2012; Gryspeerdt et al., 2018; Vergara-Temprado et al., 2018). The processes by which aerosols influence clouds depend on aerosol properties, ambient meteorology (dynamics and thermodynamics) and cloud regime (Stevens and Feingold, 2009; Andersen and Cermak, 2015; Andersen et al., 2016; Chen et al., 2016, 2018; Fuchs et al., 2018; Murray-Watson and Gryspeerdt, 2021; Zipfel et al., 2022). The effective radiative forcing due to aerosol-cloud interactions (i.e. the change in the Earth's net top-of-the-atmosphere energy flux) is estimated to be a cooling of about 1 W $m^{-2}$ (Bellouin et al., 2020; Forster et al., 2021). One of the challenges in working with satellite data to quantify aerosol-cloud interactions is that these observed aerosol-cloud relationships tend to be confounded by meteorological covariates, e.g. relative humidity or atmospheric stability, which influence both aerosols and clouds. This makes the interpretation of such aerosol-cloud relationships as causal effects difficult (Bellouin et al., 2020). Past approaches have been developed to account for this confounding by statistically accounting for confounders (Gryspeerdt et al., 2016) or including information on confounders in machine learning frameworks (Andersen et al., 2017). In a recent study, Wall et al. (2022) used an aerosol proxy from a reanalysis in a low-cloud controlling factor framework, thereby controlling for the meteorological CCFs in their forcing estimate of -1.11 W $m^{-2}$. By the addition of an aerosol proxy as a CCF in their analysis, they could predict $CRE_{SW}$ anomalies much better in so-called opportunistic experiments (e.g. for Volcanic eruptions, or in regions of known strong aerosol trends) than without the aerosol proxy. Their findings show that including additional predictors to traditional CCF frameworks can yield useful insights.

In this study, conventional regime-specific CCF frameworks are expanded upon, with a single cloud-regime independent CCF framework that uses a large number of CCFs, including various aerosol proxies from satellite observations and reanalysis. The CCF framework uses ridge regression as the statistical learning method, which enables robust sensitivity estimation in the case of many co-linear predictors. The goals of this study are 1) to develop a CCF framework to skillfully predict CRE across cloud regimes in observations, 2) to quantify and explore the regional sensitivity patterns of $CRE_{SW}$ and $CRE_{LW}$ to CCFs

https://doi.org/10.5194/egusphere-2023-1283
Preprint. Discussion started: 14 June 2023


at a global scale, and 3) quantify CRE sensitivity to various aerosol proxies. The resulting spatial patterns of sensitivity are intended to be used for future evaluations of CRE sensitivities to CCFs in global climate models and for constraining future cloud feedback estimates.

## 2 Data and methods

### 2.1 Data

All data sets described in the following cover the common time period used in this study of 2001–2020 and are monthly means regridded to a 5° x 5° spatial resolution (e.g. Scott et al., 2020; Wall et al., 2022). This is typically done in CCF analyses, as it can be assumed that at this grid scale clouds are in equilibrium with their large-scale environmental controls (Klein et al., 1995; Mauger and Norris, 2010). One should note though that this grid scale is at the upper bound of what is recommended for aerosol-cloud analyses (Grandey and Stier, 2010). Data is used over the oceans (some meteorological CCFs are only sensible choices over ocean) between 60°N and 60°S. From all data sets, the seasonality (climatological averages of each month) and linear trends are subtracted. The resulting meteorological and aerosol anomalies are then standardized by removing the mean and scaling to unit variance as in Scott et al. (2020) and Andersen et al. (2022). The set of CCFs is selected to include the most relevant drivers of cloud cover, altitude and microphysics (and thus $CRE_{SW}$ and $CRE_{LW}$s) across different cloud regimes.

Satellite observations from the polar-orbiting platform Terra are used. Short-wave and long-wave cloud radiative effects at the top of the atmosphere ($CRE_{SW}$, $CRE_{LW}$) are calculated from the gridded monthly Energy Balanced and Filled (EBAF) level 3b products, edition 4.1 from the Clouds and the Earth's Radiant Energy System (CERES) (Loeb et al., 2018) as the difference between top-of-the-atmosphere net fluxes of all-sky and (hypothetical) clear-sky conditions. The CERES EBAF data are available at a spatial resolution of 1° x 1°. Climatological means and standard deviations of $CRE_{SW}$ and $CRE_{LW}$ are shown in Fig. 1. Two commonly used proxies for CCNs are obtained from the Moderate Resolution Imaging Spectroradiometer (MODIS) sensor also mounted on the Terra platform: aerosol optical depth (AOD) and aerosol index (AI, calculated as the product of the AOD and the Ångström exponent). While AOD is sometimes still used as a CCN proxy, AI has been found better approximate CCN (Stier, 2016), giving more weight to fine mode particles (Nakajima et al., 2001). Both satellite-retrieved aerosol proxies are column-integrated, hold limited information on cloud-base CCN concentration and are known to lead to spurious aerosol-cloud relationships due to humidity-induced aerosol swelling and 3D radiative effects in the vicinity of clouds (Grandey et al., 2013; Christensen et al., 2017; Schwarz et al., 2017). Despite these limitations, in particular the AI remains a state-of-the art satellite-based CCN proxy.

Information on meteorological CCFs are taken from ERA5, the newest reanalysis product from the European Center for Medium-Range Weather Forecasts (ECMWF). The following data are used from the single-layer reanalysis (Hersbach et al., 2019b): sea-surface temperature (SST), wind speed at 10 m (WS10), mean surface latent and sensible heat fluxes (MSLHF, MSSHF), and mean sea-level pressure (MSL) (Wood, 2012; Fuchs et al., 2018; Scott et al., 2020). Data from pressure levels (Hersbach et al., 2019a) at 925, 700, 500, and 300 hPa are used for information on relative humidity (RH), air temperature (T), as well as the U, V, and vertical pressure velocity ($\omega$) components of wind (Andersen et al., 2017; Fuchs et al., 2018; Ge et al.,

https://doi.org/10.5194/egusphere-2023-1283
Preprint. Discussion started: 14 June 2023


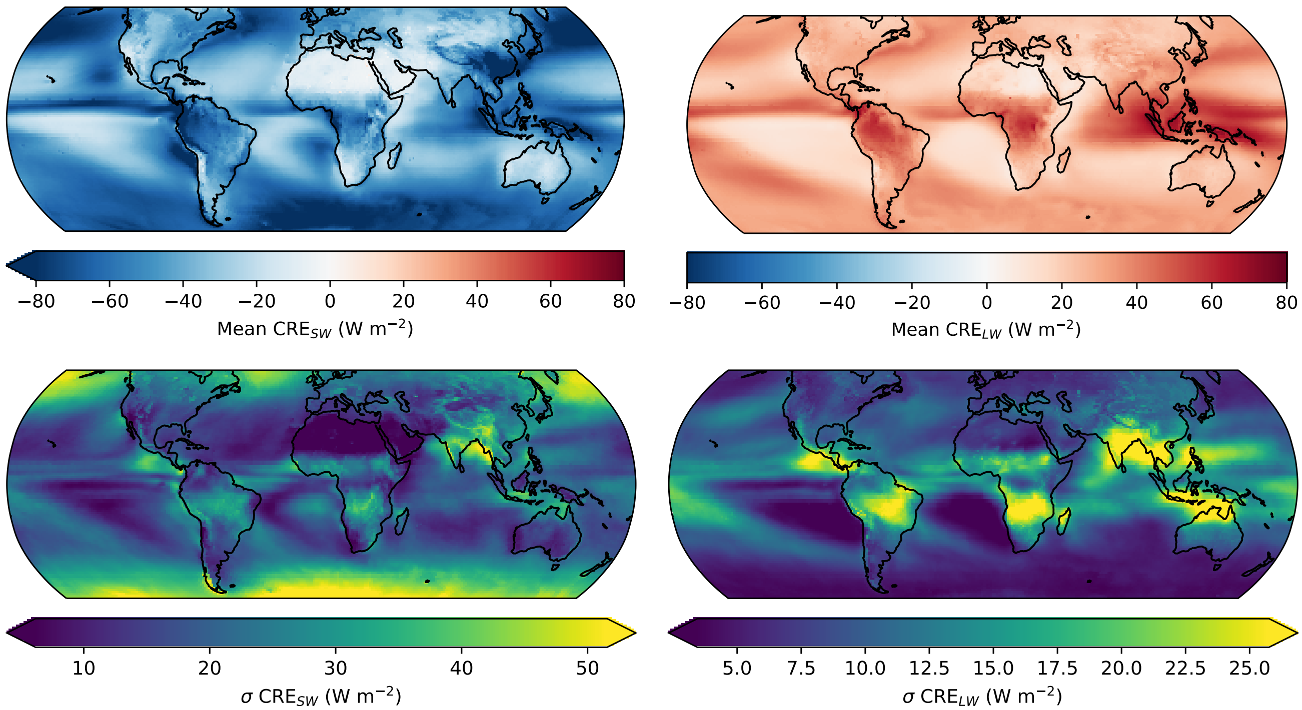


**Figure 1.** Climatological (2001–2020) mean (top) and standard deviation (bottom) of $CRE_{SW}$ (left) and $CRE_{LW}$ (right) from the CERES EBAF data.

2021; Grise and Kelleher, 2021; Kärcher, 2018; Kelleher and Grise, 2019; Patnaude et al., 2021). Data from pressure levels is referred to as $X_{zzz}$ in this paper, where X is the abbreviation of the variable name, and $_{zzz}$ the pressure level (e.g. $T_{925}$ for air temperature at 925 hPa). In addition to these CCFs, information on estimated inversion strength (EIS; (Wood and Bretherton, 2006)) and horizontal temperature advection at the surface ($T_{adv}$; (Scott et al., 2020)) is derived from ERA5 reanalysis data. The set of CCFs therefore expands upon those traditionally used for cloud-regime specific analyses (e.g. low-clouds, cf. (Scott et al., 2020)), by including information on surface fluxes, and vertically resolved proxies for dynamics (3-dimensional winds), temperature and humidity profiles to account for mechanisms controlling different cloud types and altitudes. It is assumed that the observed cloud radiative effects are a response to the CCFs chosen, even though clouds can also feedback to contribute to CCF variability (e.g. Myers et al., 2018). All data are downloaded as monthly means at the native resolution of 0.25° x 0.25°. $T_{adv}$ is the exception to this rule, as using the monthly means of the U and V wind components at 10 m (U10, V10) would lead to an underestimation of the temperature advection (because U and V can be positive and negative and a temporal average is thus closer to 0). Due to this, $T_{adv}$ is calculated from hourly U10, V10 and SST data at a spatial resolution of 2.5°x2.5° (which corresponds to the length scale of 5° as centered differencing is used for the calculation of the gradients), and then averaged to monthly means.

https://doi.org/10.5194/egusphere-2023-1283
Preprint. Discussion started: 14 June 2023


As satellite-retrieved aerosol proxies are not great proxies for CCN at cloud base (Stier, 2016) and feature the retrieval biases close to clouds discussed above, aerosol information from the MERRA-2 reanalysis are also used. The MERRA-2 aerosol reanalysis corrects the MODIS aerosol optical depth used for assimilation in the reanalysis for retrieval biases in humid environments and near clouds (Randles et al., 2017). From MERRA-2, sulfate aerosol concentrations ($s$) are used as in McCoy et al. (2017), McCoy et al. (2018) and Wall et al. (2022), by calculating monthly averages from the 3-hourly mean $s$ at 910 hPa. The data are available at a spatial resolution of 0.5° x 0.626°. As aerosol-cloud relationships tend to be linear at log-scales, the base-10 logarithm of $s$, AOD and AI are used in the statistical model (Wall et al., 2022).

### 2.2 Ridge regression

CRE$_{SW}$ and CRE$_{LW}$ anomalies are regressed on n (here: n=28) predictors so that each can be expressed as a linear combination of the local standardized CCF anomalies $X_i'$:

$$CRE' = \sum_{i=1}^{n} (\frac{\delta CRE}{\delta X_i}) * X_i' + Res$$

with Res describing a catch-all mean-zero random error term. A major challenge when using a high number $i$ of predictors X$_i$ (in particular when considering a relatively small number of samples) to predict a target variable can be co-linearity among the predictors. In classical statistical techniques (e.g. OLS), this frequently leads to high model variance (i.e. overfitting). Model variance can be reduced with regularization, which in the case of linear models is done by shrinking model coefficients towards zero by penalizing their size (Hastie et al., 2001). Ridge regression is a specific regularized linear model that makes use of the L2 penalty: the squared magnitude of the coefficient ($\beta$) value is added to the loss function, where the shrinkage is controlled by a value $\lambda$.

$$Loss_{ridge} = Error(Y - \widehat{Y}) + \lambda \sum_{1}^{n} \beta_i^2$$

Tuning the parameter $\lambda$ involves a direct trade off between a more flexible regression model (small penalty, i.e., low $\lambda$ value) that may suffer from high-variance issues, and a less flexible regression model (high penalty, high $\lambda$) that may have a larger bias. Here, the optimal  value is derived through leave-one-out cross validation by probing 1000 evenly spaced $\lambda$ values on a log scale between -3 and 5 in each 5° x 5° grid box. Leave-one-out cross validation is the default cross-validation strategy for ridge regression, as it is extremely cost efficient for least square regression (Hastie et al., 2021), and has been found to reliably find the optimal level of regularization in the case of ridge regression (Patil et al., 2021). The $\lambda$ values that lead to the best model performance in the cross validation are shown in Fig. 2. To end up with a consistent regularization, the median $\lambda$ value chosen in all cross validations (median $\lambda$ = 12 for both CRE$_{SW}$ and CRE$_{LW}$) is set fixed. This means that the final regularized models are not optimized locally, but that a representative $\lambda$ value is chosen from the cross-validations to achieve comparable model coefficients across all regions. The differences between the predictive skill in the locally optimized and $\lambda$ = 12 settings have been found to be negligible, even in regions where optimal $\lambda$ has been found to be $>$ 50. The data are split into a training

https://doi.org/10.5194/egusphere-2023-1283
Preprint. Discussion started: 14 June 2023


(2001–2015) and a test (2016–2020) set. Cross-validation and training are done based on the training data, and the model performance is evaluated based on the test data.

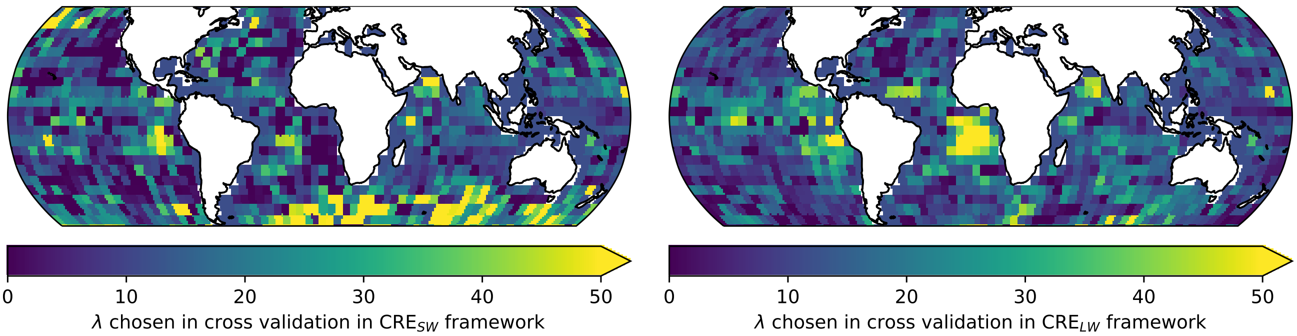


**Figure 2.** Spatial patterns of the $\lambda$ chosen in the cross validation at each grid box. The spatial median of $\lambda$ is chosen as the regularization strength for each grid box in the final model training.

Three separate CCF frameworks are trained for CRE$_{SW}$ and CRE$_{LW}$, respectively, using a different aerosol parameter each time. The meteorological sensitivities presented in this study refer to those derived from the $\log_{10}s$ setup. The regression coefficients of the ridge regression represent the sensitivity of CRE to a one standard deviation change in the local monthly anomalies in each CCF with all other local meteorological conditions held fixed, and are thus given as W m$^{-2}$ $\sigma^{-1}$(for sensitivity). As total CRE are used as a predictand (rather than specific cloud properties or CRE of a specific cloud type), the sensitivities are a top-down estimate of the total radiative response by all clouds to changes in CCFs within each grid box. Sensitivities of radiative effects of undetected very thin clouds and the transition zone between aerosols and clouds can obviously not be captured, though (Eytan et al., 2020; Jahani et al., 2021).

### 2.3 Cloud regimes

While the regression models are trained to predict CRE with the same set of CCFs independently of the region (and thus dominant cloud regime) considered, climatological cloud-regime regions are used to analyze the resulting sensitivities specifically for four regions: stratocumulus (Sc), trade cumulus (Tc), tropical ascending (Ta), and mid latitudes (Ml). The cloud regimes are defined based on climatological (2001–2020) EIS and $\omega_{700}$ thresholds similar to (Scott et al., 2020), based on Medeiros and Stevens (2011). The thresholds are given in Tab. 1, and lead to the cloud regime regions shown in Fig. 3.

## 3 Results and discussion

### 3.1 Skill of the regression models

The ridge regression models are able to capture about two thirds of the temporal variability in CRE anomalies in the independent test data, with slightly better model performance for predicting CRE$_{LW}$ than CRE$_{SW}$ (global weighted average R$^2$ of 0.72

https://doi.org/10.5194/egusphere-2023-1283
Preprint. Discussion started: 14 June 2023


**Table 1.** Thresholds to determine the cloud regime regions shown in Fig. 3.

| Cloud regime | EIS (K) | $\omega_{700}$ (hPa day$^{-1}$) |
|---|---|---|
| Sc | $> 1$ | $> 15$ |
| Tc | $< 1$ | $> 0$ |
| Ta | - | $< 0$ |
| Ml | $> 1$ | $< 15$ |

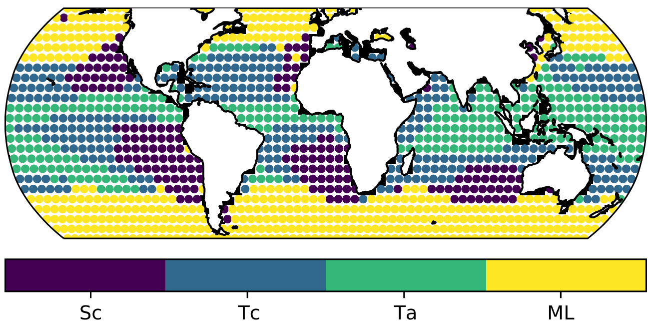


**Figure 3.** Cloud regimes derived from the EIS and $\omega_{700}$ thresholds described in Tab. 1.

vs. 0.63, standard deviation of 0.13 and 0.21, respectively). The skill is thus markedly higher than the low-cloud framework from Scott et al. (2020) (0.37, or 0.51 when information on upper-level clouds are included). This shows that the added CCFs increase the predictive performance of the model, and could indicate that they may help capture processes relevant to determine CRE, and may therefore allow for tighter constraints for cloud feedbacks and ACI than prior studies. The spatial pattern in the prediction skill of $CRE_{SW}$ shows particularly good skill in the regions of the ascending tropical cloud regime (mean $R^2 = 0.81$), and poorer performance in the mid latitudes (mean $R^2 = 0.40$), especially over the Southern Ocean. The comparably poor skill in the Southern Ocean is notable, as numerical models also have large uncertainties and biases in modeling radiative fluxes and clouds here (Gjermundsen et al., 2021; McFarquhar et al., 2021). The poor model performance may be linked to the low quality of reanalysis data sets found in this region due to the limited amount of measurements available for the assimilation (Mallet et al., 2022). The skill in predicting $CRE_{LW}$ is also highest in the tropics (mean $R^2 = 0.79$) and trade cumulus regions (mean $R^2 = 0.77$), and lower in the stratocumulus and Southern Ocean regions. This makes sense, as there is little $CRE_{LW}$ variability in those regions due to the dominance of low clouds, and hence only a small signal for the regression model to learn (see Fig. 1). Over the Southern Ocean, the assumed lower quality of the reanalysis data may also contribute to the lower skill.

There is a significant (p-value $< 0.01$) negative correlation between the prediction skill of the ridge models (Fig. 4) and the regularization strength $\lambda$ chosen in cross-validation (-0.34 for $CRE_{SW}$ and -0.31 for $CRE_{LW}$). The regularization strength that optimizes model performance is higher in regions where model performance is comparatively low. This is an indication that in these regions, the predictors do not explain the CRE variability well and that the loss during training is reduced when the

https://doi.org/10.5194/egusphere-2023-1283
Preprint. Discussion started: 14 June 2023


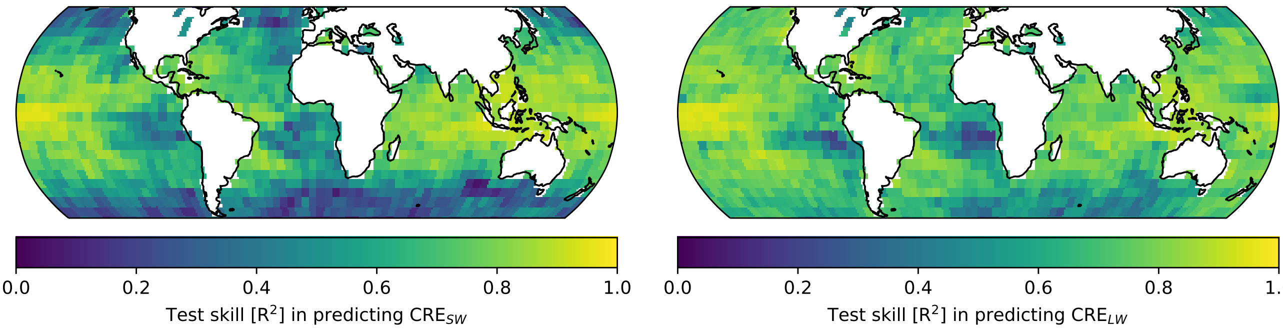


**Figure 4.** Skill ($R^2$ score) of the ridge regression models to predict $CRE_{SW}$ (left) and $CRE_{LW}$ (right) in the independent test data (2016–2020).

model sensitivities are smaller (thereby predicting less CRE variability). Coefficients of selected CCFs estimated by the ridge regression are described in the following, with the focus on 1) SST and EIS as well-known low-cloud CCFs important for the low-cloud feedback, 2) 3-dimensional winds at different pressure levels for information on large-scale dynamics that are often not part of CCF frameworks and 3) aerosol proxies, as a way of analyzing ACI in a CCF framework.

### 3.2 Sensitivity of $CRE_{SW}$ and $CRE_{LW}$ to SST and EIS

SST and EIS are the two main drivers of the marine low-cloud feedback (Myers and Norris, 2016; Myers et al., 2021; Klein et al., 2017; Cesana and Del Genio, 2021), and are thus discussed first. The overall sensitivity of CRE to SST is dominated by the positive sensitivity of $CRE_{SW}$ (global weighted mean = 1.11 W m$^{-2}$ $\sigma^{-1}$, compared to -0.12 W m$^{-2}$ $\sigma^{-1}$for $CRE_{LW}$). The $CRE_{SW}$ sensitivity is particularly high in the stratocumulus regime (1.64 W m$^{-2}$ $\sigma^{-1}$), which is to be expected, as these clouds are more strongly coupled to surface processes than e.g. cumulus clouds in the trades (Wood, 2012; Cesana et al., 2019; Scott et al., 2020; Cesana and Del Genio, 2021). SST can influence low clouds via different mechanisms. Surface latent heat fluxes increase with SST, which enhances the buoyancy within the marine boundary layer and deepens it, leading to an increased entrainment of dry free-tropospheric air and thus evaporation of cloud water (Rieck et al., 2012; Qu et al., 2015). Also, increases in SST can lead to a stronger vertical moisture gradient, making dry-air entrainment more efficient in evaporating cloud (as the entrained air is relatively drier compared to the marine boundary layer air, (Qu et al., 2015; van der Dussen et al., 2015)), which has been shown to be the main cause of the recent decrease in low clouds off the coast of California (Andersen et al., 2022) where the SST-$CRE_{SW}$ sensitivity is found to be largest. These findings generally agree with those of Scott et al. (2020) who specifically analyze low-cloud induced changes in radiative fluxes, although their average sensitivity estimate is lower and not positive in all regions. $CRE_{LW}$ sensitivities are in general negligible for the stratocumulus cloud regime, as their warm cloud tops only induce a minor $CRE_{LW}$. There is a systematic negative $CRE_{LW}$-SST sensitivity in the Tc regime (-0.29 W m$^{-2}$ $\sigma^{-1}$), which is outweighed by the positive $CRE_{SW}$-SST sensitivity in that regime, though (1.08 W m$^{-2}$ $\sigma^{-1}$). In the tropics, there is a band of moderate positive $CRE_{LW}$-SST sensitivity, indicative of more frequent or higher-reaching

https://doi.org/10.5194/egusphere-2023-1283
Preprint. Discussion started: 14 June 2023


convection in cases of higher SSTs. While such local effects of SST on deep convection have been noted in the past (Zhang, 1993), non-local pattern effects of SST on deep convective CRE (Fueglistaler, 2019) cannot be captured with our approach.

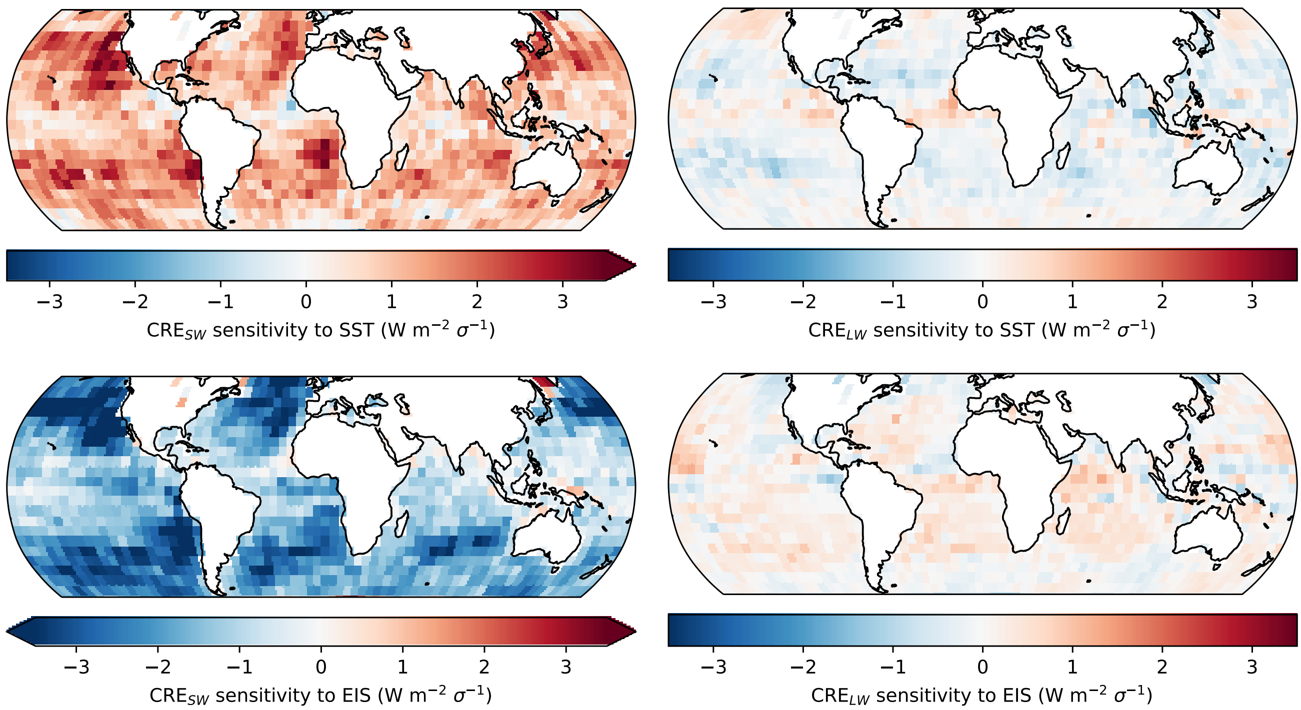


**Figure 5.** Sensitivity of $CRE_{SW}$ (left) and $CRE_{LW}$ (right) to SST (top) and EIS (bottom).

The sensitivity of CRE to EIS is dominated by the negative $CRE_{SW}$ sensitivity (global weighted mean = -1.57 W m$^{-2}$ $\sigma^{-1}$), which is also particularly strong in the Sc regime (-2.33 W m$^{-2}$ $\sigma^{-1}$) and the Ml (-1.97 W m$^{-2}$ $\sigma^{-1}$) and smallest for the Ta regime (-0.91 W m$^{-2}$ $\sigma^{-1}$). The results agree remarkably well with those found by Scott et al. (2020) both in overall magnitude and spatial/regime patterns. EIS modifies low clouds by controlling the amount of dry-entrainment from the free troposphere into the marine boundary layer, where a strong inversion limits this entrainment and leads to a shallower marine boundary layer effectively trapping moisture. This has been observed particularly in the Sc and Southern Ocean regimes (Klein and Hartmann, 1993; Wood and Bretherton, 2006; Kelleher and Grise, 2019; Scott et al., 2020). There is only a limited, mainly positive sensitivity of $CRE_{LW}$ to EIS, which is largest in the Tc regime (0.24 W m$^{-2}$ $\sigma^{-1}$). This is due to the moderate LW warming exerted by an increase in Tc clouds. The overall low magnitude of the $CRE_{LW}$ to EIS is expected, as similar to SST, EIS mainly drives low-cloud variability.

https://doi.org/10.5194/egusphere-2023-1283
Preprint. Discussion started: 14 June 2023


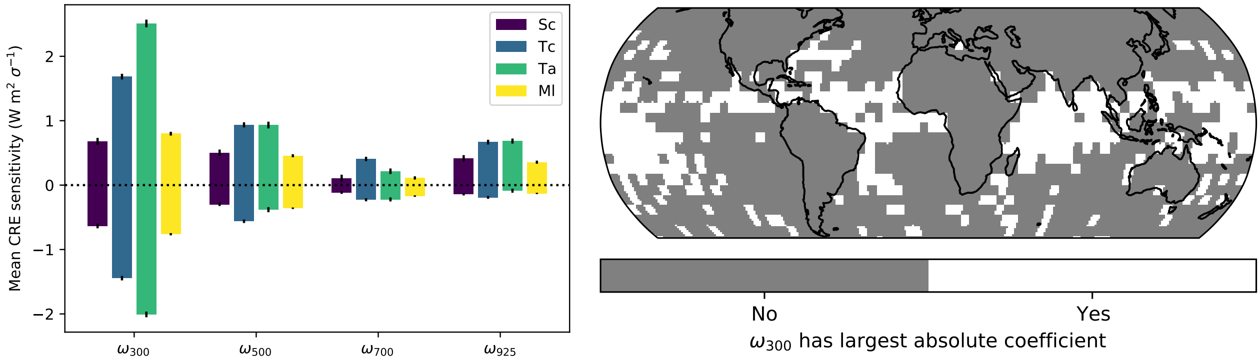


**Figure 6.** Left: Mean CRE sensitivity to $\omega$ at different pressure levels and for different cloud regime regions (denoted by the color). CRE sensitivities that are positive are always from $CRE_{SW}$, negative ones from $CRE_{LW}$. The error bars denote the standard error of the mean value ($\sigma/\sqrt{n}$) with n = sample size. Right: Map showing the regions where $\omega_{300}$ has the largest absolute coefficient for $CRE_{SW}$.

### 3.3 Sensitivity of $CRE_{SW}$ and $CRE_{LW}$ to large-scale circulation

Variability in large-scale circulation and dynamics are mainly approximated by anomalies in the 3-dimensional winds at different pressure levels (300, 500, 700, and 925 hPa). The sensitivity of CRE to variations in the vertical pressure velocity $\omega$ is largest at 300 hPa, which is the strongest predictor for CRE in general in the ascending tropics (Fig. 6). The sensitivity of $CRE_{SW}$ and $CRE_{LW}$ are nearly balanced for $\omega_{300}$, but less so for $\omega_{925}$, where $\omega$ within the boundary layer mostly influences low clouds and thus $CRE_{SW}$. In the free troposphere at 700 hPa, $\omega$ is only a minor control of CRE variability. The sensitivity patterns of $CRE_{SW}$ and $CRE_{LW}$ (Fig. 7) closely follow the regions of tropical ascent, and reach maximum values in the tropical warm pool region. In the Ta regime, $\omega_{300}$ anomalies are shown to lead to a strong cooling from the $CRE_{SW}$ (2.51 W m$^{-2}$ $\sigma^{-1}$) that is nearly completely balanced by a strong warming from the $CRE_{LW}$ (-2.01 W m$^{-2}$ $\sigma^{-1}$) by the increase in upper-level clouds. While the nearly exact opposite mirroring of the CRE sensitivity patterns to $\omega_{300}$ (correlation coefficient = -0.86 globally and -0.81 in the Ta regime) can partly be explained by the overall balance of $CRE_{SW}$ and $CRE_{LW}$ in this region (Fig. 1), it is noteworthy, since the cancellation of $CRE_{SW}$ and $CRE_{LW}$ is the result of a mixing of various cloud types with very specific CRE signatures (Wall et al., 2019). This seems to confirm that $\omega_{300}$ is a strong predictor for the occurrence of most (deep) convective and cirrus clouds that dominate the CRE in the Ta regime (Ge et al., 2021).

CRE sensitivity to variability in zonal and meridional winds is most pronounced at 700 hPa and in the subtropics. The sensitivities to $U_{700}$ and $V_{700}$ anomalies (Fig. 8) are not trivial to understand, as they can be related to a change in wind speed or direction, dependent on the sign and climatological average of the wind component. In the following, these controlling factors are therefore explored in more detail.

$CRE_{SW}$ is markedly sensitive to $U_{700}$ in the core stratocumulus regions (mean Sc 1.05 W m$^{-2}$ $\sigma^{-1}$), where clouds are typically below that level (Zuidema et al., 2009). As the stratocumulus clouds do not have a marked $CRE_{LW}$, this pattern only exists for the $CRE_{SW}$. In these regions, a positive $U_{700}$ $CRE_{SW}$ sensitivity suggests a decrease in cloudiness with a westerly

https://doi.org/10.5194/egusphere-2023-1283
Preprint. Discussion started: 14 June 2023


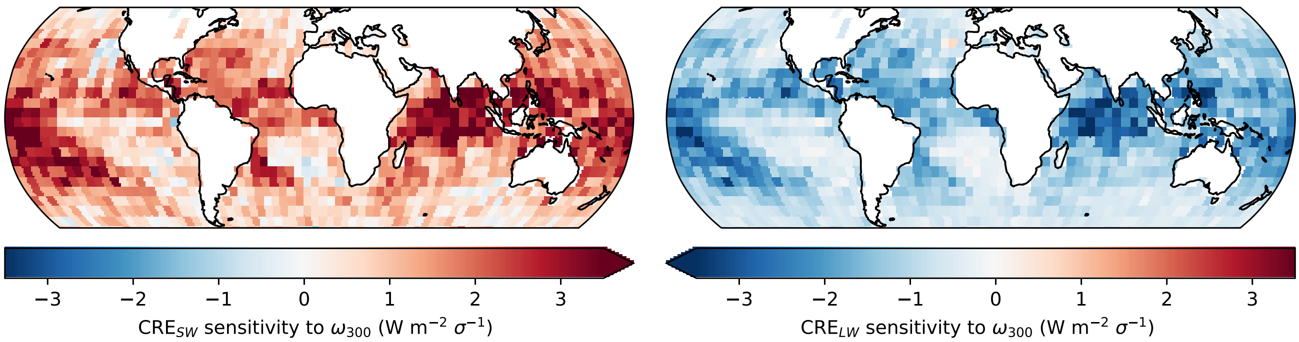


**Figure 7.** Sensitivity of CRE$_{SW}$ (left) and CRE$_{LW}$ (right) to $\omega_{300}$.

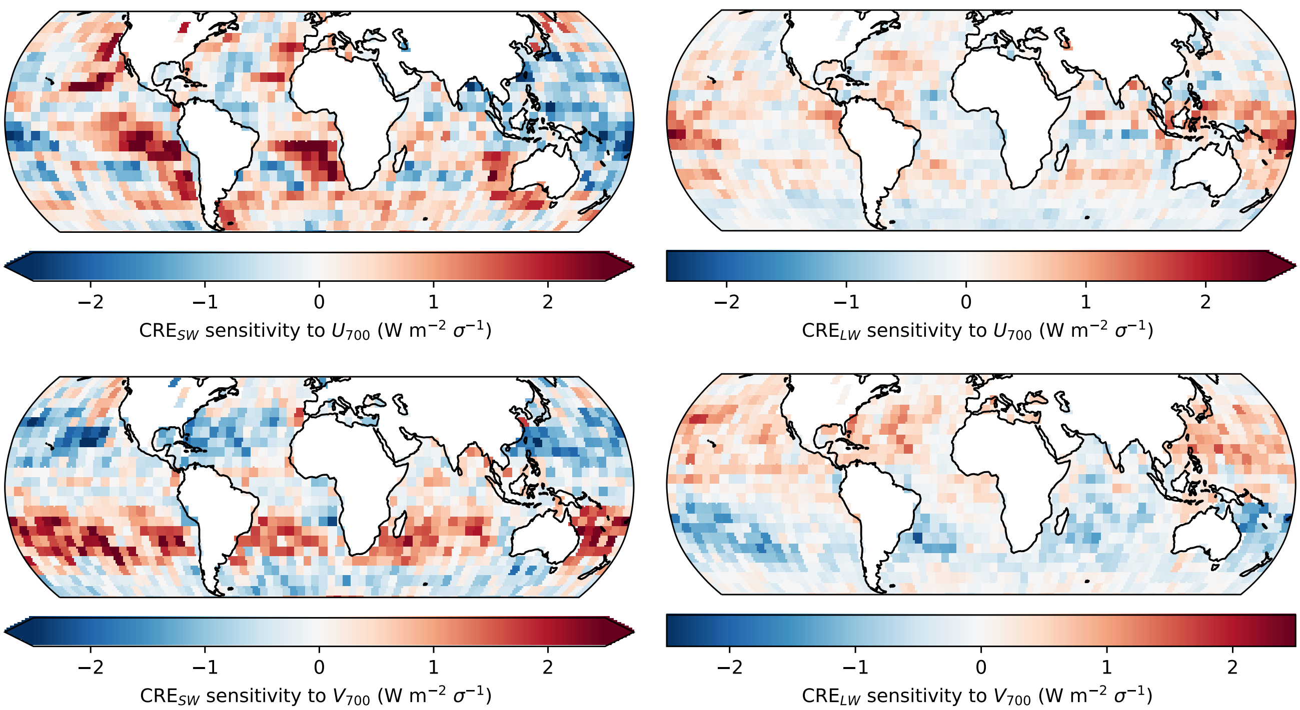


**Figure 8.** Sensitivity of CRE$_{SW}$ and CRE$_{LW}$ to U$_{700}$ and V$_{700}$. Note the smaller sensitivity range in the colorbar when compared to Fig. 5 and Fig. 7 (-2.5–2.5 vs. -3.5–3.5).

anomaly of the wind at 700 hPa. The opposite is the case over a trade wind cumulus region of the tropical pacific, even though the sensitivity is less pronounced. In the following, a composite analysis is used to better understand what drives variability of local U$_{700}$ and how that may be related to CRE in an exemplary subtropical low-cloud region. Fig. 9 shows the composite of anomalies in CCFs when U$_{700}$ anomalies in the Southeast Atlantic at 17.5°S and 2.5°E (black "x") are $> 1\ \sigma$. The top left panel

https://doi.org/10.5194/egusphere-2023-1283
Preprint. Discussion started: 14 June 2023


shows MSL anomalies which feature a high pressure anomaly over the midlatitudinal Atlantic that strongly modifies the free-tropospheric winds. As the climatological mean boundary layer flow in the Southeast Atlantic is from a southeasterly direction, a northwesterly anomaly in the free-troposphere flow tends to increase the vertical wind shear at the top of the boundary layer (u-wind shear between 700 and 925 hPa shown in the top center panel of Fig. 9). In a stratocumulus-topped boundary layer an increased vertical wind shear is known to cause additional turbulence at the cloud top, and lead to stronger entrainment of dry air into the cloudy marine boundary layer. A stronger dry-air entrainment would then dissolve the clouds from the top (Kopec et al., 2016; Zamora Zapata et al., 2021). The boundary layer humidity ($RH_{925}$) is markedly increased in the composite along the south-western African coastline (top right), which would presumably lead to an increase in cloudiness as well (contrary to what is observed). While a synoptically-driven destabilization (reduced EIS) has also been reported to influence low-level clouds in this region (de Szoeke et al., 2016; Fuchs et al., 2017), and can also be observed here (bottom left), this spatial anomaly pattern does not match the cloud field anomaly and can thus not explain the decrease in local cooling from $CRE_{SW}$. The bottom right panel shows the average ridge regression contributions of the most important CCFs to the predicted local $CRE_{SW}$ anomaly of the composite analysis (multiplying the average standardized anomaly of the composite times the coefficients at the marked "x" location). Overall, the observed local $CRE_{SW}$ anomaly of these situations of 5.41 W $m^{-2}$ can be reproduced fairly well by the ridge regression model, even though it is somewhat underestimated (3.85 W $m^{-2}$). It is clear that in these situations, $U_{700}$ has the largest contribution (4.51 W $m^{-2}$) to the predicted $CRE_{SW}$ anomaly, which cannot be explained by the other CCFs. The humidification of the boundary layer has the strongest negative contribution to the predicted $CRE_{SW}$ anomaly (-2.22 W $m^{-2}$; increase in clouds), partly balancing the $U_{700}$ contribution. While vertical wind shear was not originally considered as a CCF in the model, at this location in the Southeast Atlantic, vertical wind shear and $U_{700}$ are strongly correlated (-0.90), which is also the case in all stratocumulus regions (average correlation for the Sc regime: -0.74), so that in these regions, $U_{700}$ can be thought of as a proxy for vertical wind shear. Based on these results, the wind-shear induced turbulence at cloud top leading to entrainment and low-cloud dissipation is likely the main cause for the observed decrease in cooling from low-clouds (bottom center) associated with these conditions of the composite analysis, and for the observed sensitivity of $CRE_{SW}$ to $U_{700}$ anomalies in the Sc regime. As such, vertical wind shear is recommended to be further explored in CCF analysis, especially for low cloud frameworks.

There is a coherent subtropical belt of a marked sensitivity of CRE to $V_{700}$ between $\approx$15° and 35° with maximum sensitivity values between 20° and 25° in each hemisphere (Fig. 8, bottom). The sensitivity has opposite signs depending on the hemisphere and the radiative effect considered, and describes an increase in the cooling ($CRE_{SW}$) or warming ($CRE_{LW}$) effect of clouds connected to a poleward anomaly of the winds at 700 hPa. The zonal structure of the $CRE_{SW}$ and $CRE_{LW}$ sensitivities to $V_{700}$ is clearly visible in Fig. 10a). Fig. 10b) and c) show a clear connection of poleward $V_{700}$ anomalies with large scale ascent at the same pressure level and an increase in shortwave cooling from clouds (and vice versa). To give this finding more context, two composite analyses of situations with $V_{700} > 1\,\sigma$ in the South Atlantic and South Pacific regions are discussed in the following.

Fig. 11 shows a connection of the conditions with $V_{700}$ anomalies $> 1\sigma$ to a subtropical low pressure anomaly that is linked to a midlatitude synoptic-scale disturbance. The local poleward flow anomaly is clearly connected to a large-scale

https://doi.org/10.5194/egusphere-2023-1283
Preprint. Discussion started: 14 June 2023


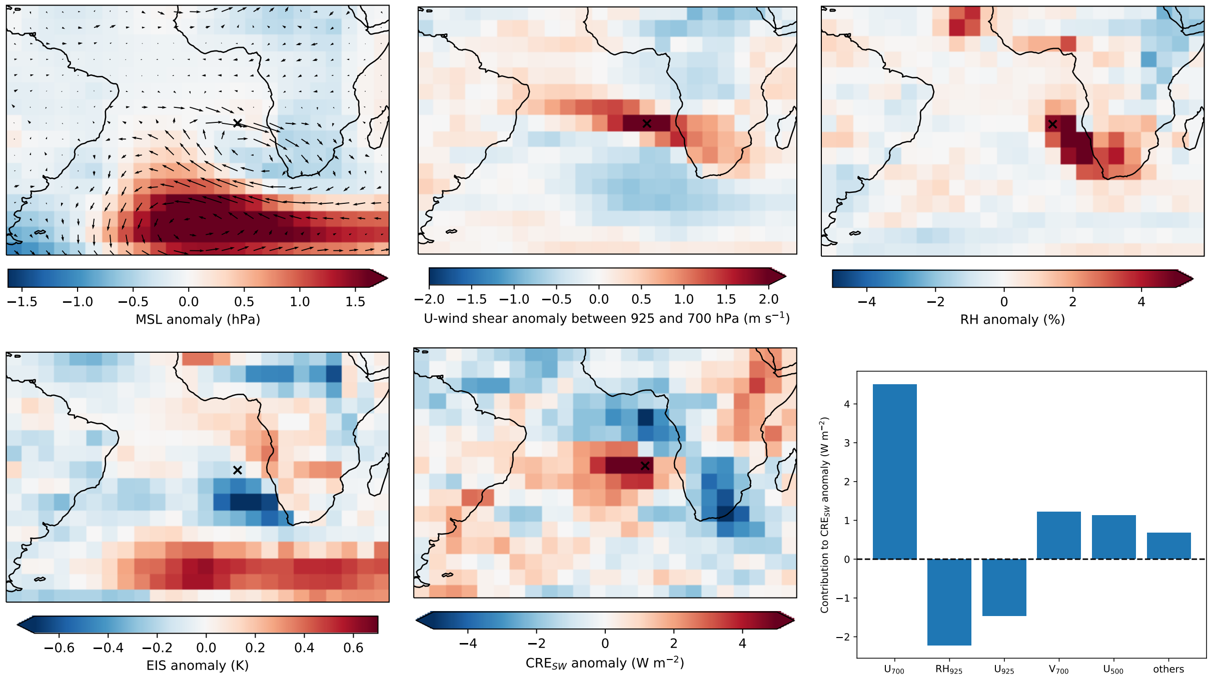


**Figure 9.** Composite analysis of anomalies in CCFs and $CRE_{SW}$ when $U_{700}$ anomalies in the Southeast Atlantic at 17.5°S and 2.5°E (black "x") $> 1\sigma$. The panel in the top left shows MSL anomalies and wind anomalies at 700 hPa, and the top center panel shows the wind shear anomaly of the u-component between the boundary layer (925 hPa) and the free troposphere (700 hPa). The top right panel shows the RH anomaly in the bounday layer (925 hPa). The bottom left panel shows EIS anomalies, and the bottom center panel shows the observed $CRE_{SW}$ anomalies. The panel in the bottom right shows the ridge-regression quantified contributions of selected CCFs and the sum of all others to the predicted $CRE_{SW}$.

ascent anomaly which is causing an increase in humidity and clouds/decrease in $CRE_{SW}$, confirming the observed correlations between $V_{700}$, $\omega_{700}$ and $CRE_{SW}$ presented in Fig. 10. While it is generally known that ascending air is the main mechanism by which air is saturated and clouds form, a positive association between low clouds and free-tropospheric ascent has also been found in subtropical regions of climatological subsidence (Myers and Norris, 2013). The results from this exemplary composite analysis are indicative of the poleward and upward vertical velocity phases of synoptic waves/midlatitude cyclones and the associated increase in cloudiness. The ridge-regression can reproduce the local $CRE_{SW}$ anomalies for these composites well (observed vs. predicted: Atlantic -7.37 vs. -6.36, Pacific -12.74 vs. -12.28 W m$^{-2}$), and the quantified contributions to the predicted $CRE_{SW}$ anomalies (bottom panels) show that indeed, the largest contributions come from $\omega$ and RH at different levels in the free troposphere, and from $V_{700}$. There are two possible explanations for the CRE sensitivity to $V_{700}$: 1) The physical explanation: The enhanced poleward winds on the eastern side of the midlatitude cyclones could be related to increased warm and moist advection, which increases cloudiness. 2) The statistical explanation: $V_{700}$ anomalies are correlated to large-scale ascent which is causing the clouds to form and additionally have a high signal-to-noise ratio for such midlatitude synoptic

https://doi.org/10.5194/egusphere-2023-1283
Preprint. Discussion started: 14 June 2023


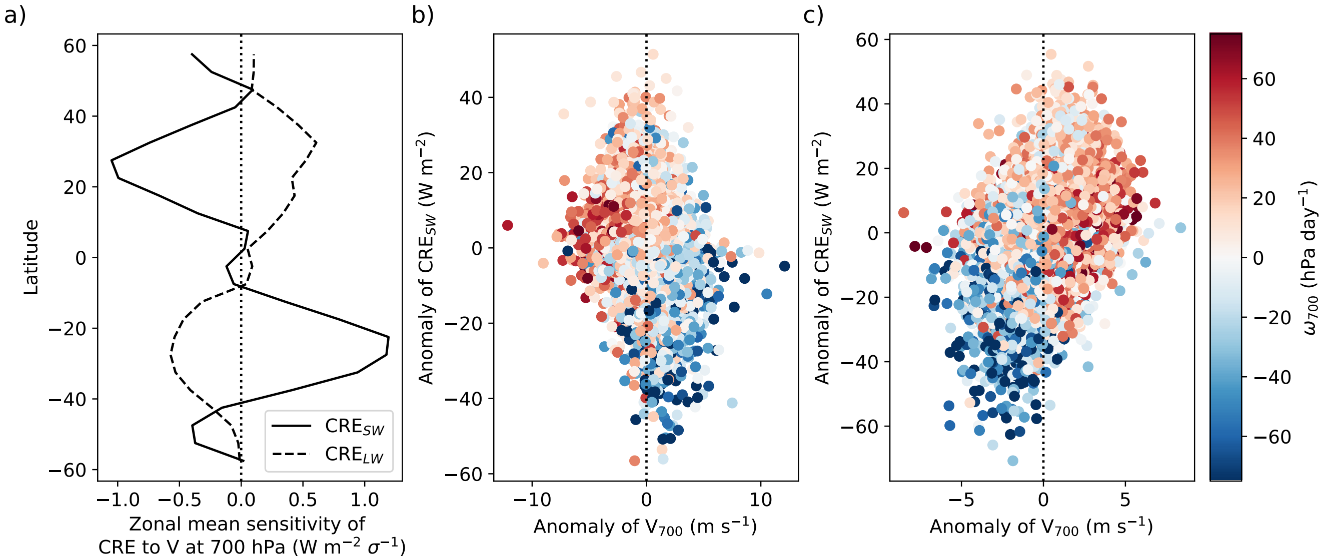


**Figure 10.** Summary of the CRE sensitivity to $V_{700}$ anomalies. a) Zonal mean sensitivities of $CRE_{SW}$ (solid line) and $CRE_{SW}$ (dashed line) point to strong sensitivities in the subtropics. b)/c) show the $CRE_{SW}$ anomaly against the $V_{700}$ anomalies in the Northern (centre panel) and Southern (right-hand panel) Hemisphere where the sensitivity exceeds |1.5| W $m^{-2}$ $\sigma^{-1}$, with the color showing $\omega_{700}$ (blue: ascent, red: subsidence).

variability. By capturing this synoptic variability, $V_{700}$ anomalies would then encapsulate changes in a number of relevant CCFs (not only $\omega_{700}$) related to the synoptic forcing, and thereby be assigned the observed sensitivities. In this regard, it should be noted that an anomaly pattern similar to that of $\omega_{700}$ can also be found for $\omega$ at 500 and 300 hPa, showing that the disturbance leads to vertically extended large-scale ascent. The question is to what degree the $V_{700}$ sensitivity and resultant contributions are a result from a physical connection between $V_{700}$ and $CRE_{SW}$ in the subtropical belts or from the correlation of $V_{700}$ with ascending motion that is driving cloudiness, but cannot directly be answered with this approach, highlighting the challenge of trying to untangle causality with statistical models and correlated inputs. The coherent association of $V_{700}$ anomalies and $\omega_{700}$ (see Fig. 10) suggests that the composite analyses are likely representative for other regions in the subtropical $V_{700}$ sensitivity belt as well.

### 3.4 Sensitivity patterns of $CRE_{SW}$ and $CRE_{LW}$ to aerosol proxies

CRE sensitivities to three different aerosol proxies ($\log_{10}s$, $\log_{10}$AI, and $\log_{10}$AOD) are described in the following. It should be noted that changing a CCF (here: the aerosol proxy) slightly changes other sensitivities as well. The magnitude of these changes depends on the aerosol proxies compared. Fig. 12 shows the correlation of spatial sensitivity patterns among individual CCFs for different aerosol proxy combinations. It can be seen that when the two satellite-derived aerosol proxies are compared, all other sensitivity patterns stay nearly constant (average correlation = 0.99 and 0.98 for $CRE_{SW}$ and $CRE_{LW}$, respectively), and

https://doi.org/10.5194/egusphere-2023-1283
Preprint. Discussion started: 14 June 2023


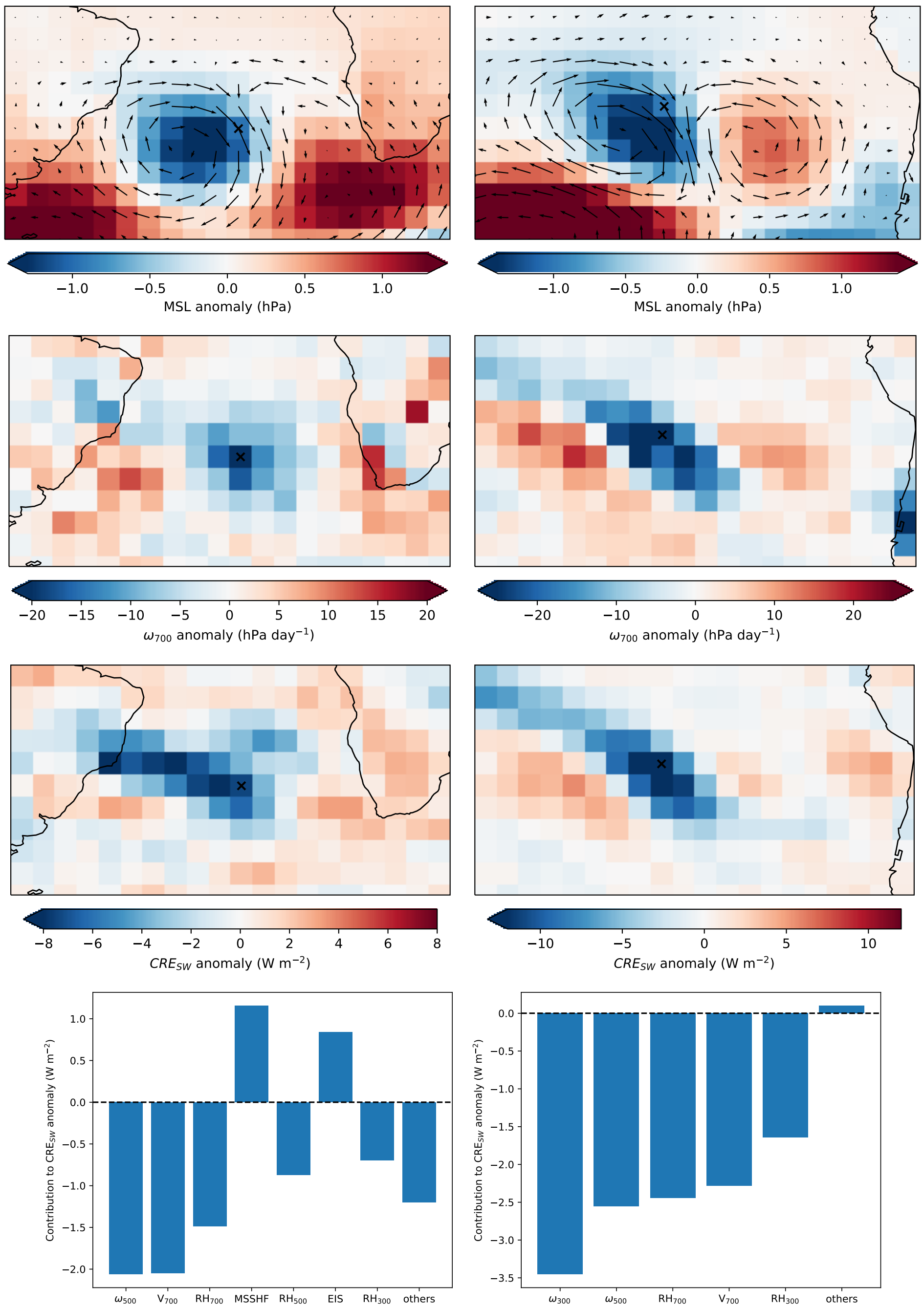


**Figure 11.** Composite analysis of anomalies in CCFs and $CRE_{SW}$ when $V_{700}$ in the Southeast Atlantic (left: at 27.5°S and 12.5°W) and in the South Pacific (right: at 22.5°S and 127.5°W) $> 1\sigma$. From top to bottom, the panels show MSL anomalies and wind anomalies at 700 hPa, $\omega_{700}$ anomalies, observed $CRE_{SW}$ anomalies, and ridge-regression quantified contributions to the predicted $CRE_{SW}$ anomaly.

https://doi.org/10.5194/egusphere-2023-1283
Preprint. Discussion started: 14 June 2023


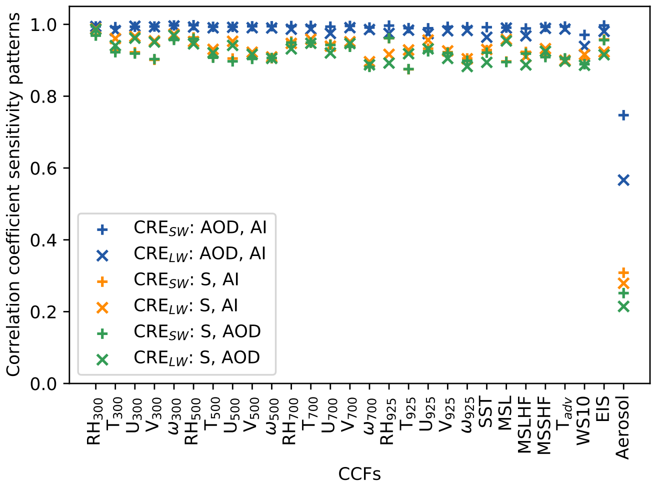


**Figure 12.** Correlation of spatial sensitivity patterns of all individual CCFs estimated by ridge regression models for different aerosol proxy pairs as noted in the legend. In this study only CRE sensitivities to meteorological CCFs from the $\log_{10}s$ are shown.

the derived spatial sensitivity patterns of $\log_{10}$AOD and $\log_{10}$AI are fairly strongly correlated as well. This is not surprising, as AOD and AI are directly related. In sensitivity estimates that use $\log_{10}s$ as an aerosol proxy correlations amongst the other CCF sensitivity patterns are lower (on average $\approx$ 0.92–0.93), and the CRE $\log_{10}s$ sensitivities are not strongly correlated to those of the satellite-derived aerosol proxies (0.21–0.31). When comparing the sensitivity patterns of the aerosol proxies in the following, the different nature of the aerosol data sets should be kept in mind: The satellite-derived AOD and AI are columnar retrievals, do not focus on a specific aerosol species and suffer from retrieval biases close to clouds (especially the AOD), while the sulfate concentration from the aerosol reanalysis focuses on a single species at a level close to cloud base (for clouds forming in the marine boundary layer), and is expected to have reduced biases typical of satellite retrievals. However, the aerosol reanalysis may introduce different model-based biases, which are not well known. In regions where sulfate does not dominate CCN, $\log_{10}s$ is not expected to be a good proxy for CCN at cloud base.

The left-hand column of Fig. 13 shows CRE$_{SW}$ sensitivity to the three aerosol proxies. It is apparent that all aerosol proxies feature a negative global weighted average sensitivity, with that of $\log_{10}s$ being markedly smaller in magnitude (-0.17 W m$^{-2}$ $\sigma^{-1}$) than those of $\log_{10}$AI (-0.25 W m$^{-2}$ $\sigma^{-1}$) and $\log_{10}$AOD (-0.34 W m$^{-2}$ $\sigma^{-1}$). Similar to the recent study by Wall et al. (2022) who explored the effects of $\log_{10}s$ in a low-cloud-specific CCF framework, and other recent global studies (e.g. Hasekamp et al., 2019; Toll et al., 2019; Jia et al., 2021) sensitivities are strongest in the Sc regime with CRE$_{SW}$ sensitivity to $\log_{10}s$ of -0.43 W m$^{-2}$ $\sigma^{-1}$, to $\log_{10}$AOD of -0.70 W m$^{-2}$ $\sigma^{-1}$, and to $\log_{10}$AOD of -0.66 W m$^{-2}$ $\sigma^{-1}$. A marked difference between the derived sensitivity patterns is that in the Ta regime, the CRE$_{SW}$ sensitivity to $\log_{10}s$ is negligible (-0.06 W m$^{-2}$ $\sigma^{-1}$), whereas it is substantial for $\log_{10}$AI (-0.27 W m$^{-2}$ $\sigma^{-1}$) and even larger for $\log_{10}$AOD (-0.50 W m$^{-2}$ $\sigma^{-1}$). In general, the finding of a stronger sensitivity for the satellite-derived aerosol proxies is expected, in particular in the case of AOD, due to the retrieval issues discussed in Section 2.1. While the ridge regression does control for the large-scale meteorol-

https://doi.org/10.5194/egusphere-2023-1283
Preprint. Discussion started: 14 June 2023


ogy, the sensitivity is likely to still be confounded for the satellite-derived aerosol proxies, as aerosol swelling can be expected to affect aerosol retrievals at much smaller scales.

The right-hand column of Fig. 13 shows the sensitivity patterns of $\mathrm{CRE}_{LW}$ to the different aerosol proxies, with a positive global weighted mean sensitivity for all proxies ($\log_{10}s$: 0.05 W m$^{-2}$ $\sigma^{-1}$, $\log_{10}$AI: 0.03 W m$^{-2}$ $\sigma^{-1}$, and $\log_{10}$AOD: 0.44 W m$^{-2}$ $\sigma^{-1}$). While the $\mathrm{CRE}_{LW}$ sensitivity is much smaller than the $\mathrm{CRE}_{SW}$ sensitivity for $\log_{10}s$ and $\log_{10}$AI, this is not the case for $\log_{10}$AOD, especially in the Ta regime, where the sensitivity is large (0.87 W m$^{-2}$ $\sigma^{-1}$). This is likely due to the (largely spurious) relationships between AOD and cloud fraction (Gryspeerdt et al., 2016; Andersen et al., 2017; Christensen et al., 2017) and cloud-top temperature (Gryspeerdt et al., 2014) that dominate the $\mathrm{CRE}_{LW}$ signal. It is notable that while $\log_{10}$AI produces a similar overall sensitivity pattern (correlation = 0.57, see Fig. 12), the magnitude is lower by a factor of 17 in the Ta regime. Overall, $\mathrm{CRE}_{LW}$ sensitivity to aerosol proxies is large where the $\mathrm{CRE}_{SW}$ is large as well (correlations are -0.49 for $\log_{10}s$, -0.53 for $\log_{10}$AI, -0.69 for $\log_{10}$AOD), indicating that a large fraction of the quantified aerosol sensitivity is from the cloud adjustments that influence both $\mathrm{CRE}_{SW}$ and $\mathrm{CRE}_{LW}$. In that sense it is expected that the correlation between the $\mathrm{CRE}_{SW}$ and $\mathrm{CRE}_{LW}$ sensitivity is particularly large for $\log_{10}$AOD, as it is particularly sensitive to aerosol swelling (thus spuriously relating AOD and cloud fraction). In the future, to better understand the differences in aerosol proxy-CRE relationships, a decomposition into cloud amount and radiative property changes of clouds maybe helpful.

## 4 Summary and conclusions

In this study, a regime-independent CCF framework was presented to predict near-global $\mathrm{CRE}_{SW}$ and $\mathrm{CRE}_{LW}$. A regularized linear statistical learning technique (ridge regression) was used to quantify sensitivities of $\mathrm{CRE}_{SW}$ and $\mathrm{CRE}_{LW}$ to 28 CCFs, including three different aerosol proxies. The quantified sensitivities are investigated for selected CCFs, and in regions of four broad cloud regimes. The most relevant findings are described in the following.

1. The statistical models are shown to be able to skillfully predict $\mathrm{CRE}_{SW}$ (global average $R^2$ = 0.63) and $\mathrm{CRE}_{LW}$ ($R^2$ = 0.72) in independent test data. Model skills are highest in the tropics, and lower at high latitudes and in particular the Southern Ocean.

2. The sensitivity of CRE to the two most dominant low-cloud controls, SST and EIS, is most pronounced in the shortwave. It is strongest in regions where stratocumulus clouds dominate and largely consistent with other studies, suggesting an increase in low clouds with increasing EIS and decreasing SST.

3. In the tropics, $\omega_{300}$ is the most important CCF, influencing $\mathrm{CRE}_{SW}$ and $\mathrm{CRE}_{LW}$ in such a way that the effects of $\omega_{300}$ nearly cancel out.

4. Zonal and meridional winds in the free troposphere are shown to be important proxies for synoptic variability relevant for subtropical CREs. Increases in $U_{700}$ anomalies due to midlatitude synoptic variability are shown to be associated with a reduced cooling from clouds in stratocumulus regions. $U_{700}$ anomalies are shown to be a good proxy for changes in vertical wind shear between the boundary layer and the free troposphere and thus the generation of turbulence at cloud

https://doi.org/10.5194/egusphere-2023-1283
Preprint. Discussion started: 14 June 2023


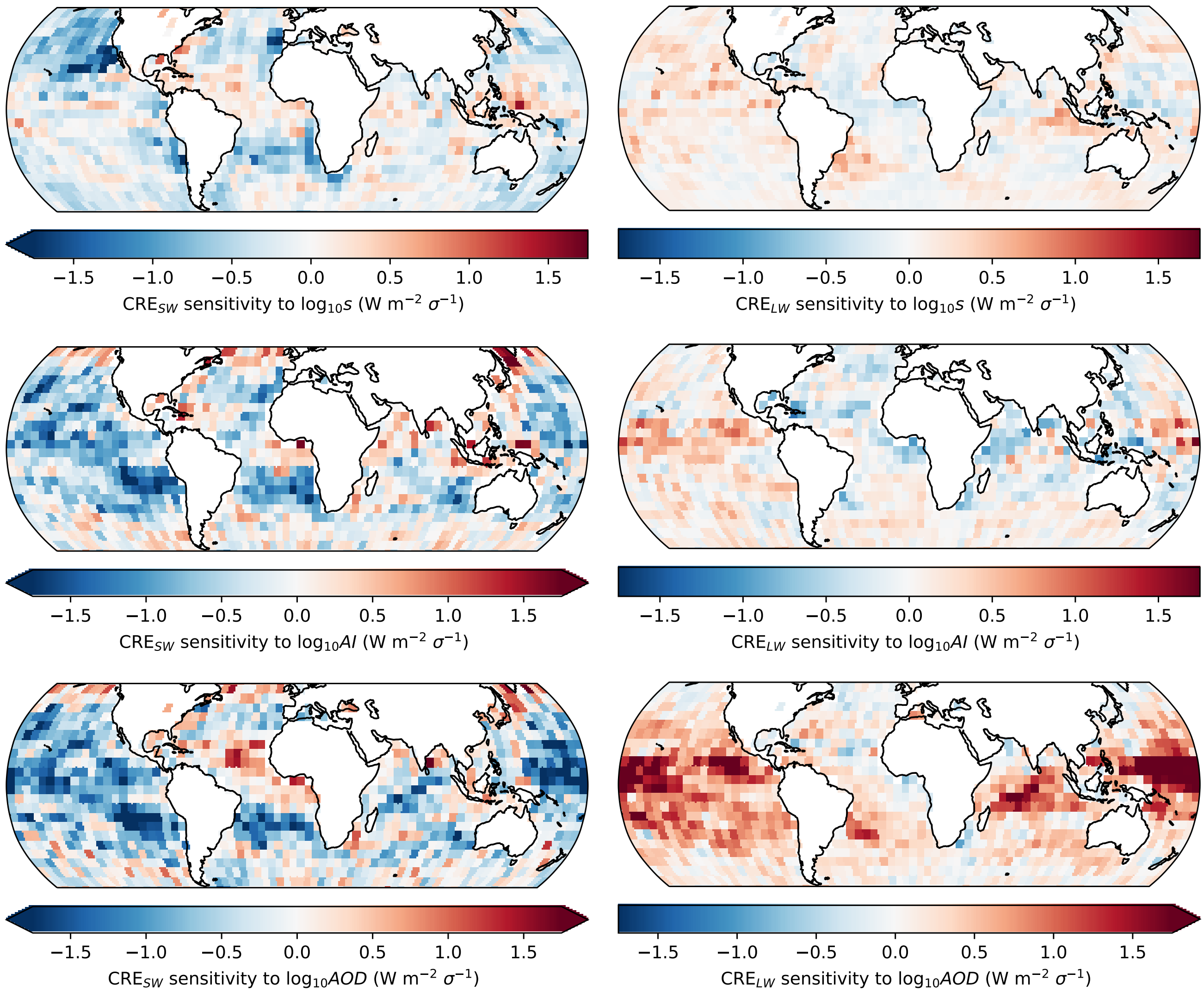


**Figure 13.** Sensitivity of CRE$_{SW}$ (left) and CRE$_{LW}$ (right) to $\log_{10}s$ (top), $\log_{10}$AI (centre), and $\log_{10}$AOD (bottom). Note that a smaller sensitivity range is shown compared to the other sensitivity maps.

https://doi.org/10.5194/egusphere-2023-1283
Preprint. Discussion started: 14 June 2023


top, leading to the depletion of low-clouds. Vertical wind shear should thus be included and explored in CCF frameworks, in particular in low cloud studies. CRE is sensitive to $V_{700}$ in the subtropics, where poleward $V_{700}$ anomalies are linked to increased cooling from clouds. It is unclear though, to what degree the $V_{700}$ sensitivity is related to warm, moist meridional advection that may increase cloudiness or driven by the correlation of $V_{700}$ with large-scale ascent in the region which may lead to nonphysical statistical associations. The analysis highlights the difficulty in assessing causality in a statistical model with correlated inputs.

5. The CRE sensitivities to the three aerosol proxies ($\log_{10}s$, $\log_{10}$AI, and $\log_{10}$AOD) share the average sign (negative for $\mathrm{CRE}_{SW}$ and positive for $\mathrm{CRE}_{LW}$), and have some qualitative similarities ($\mathrm{CRE}_{SW}$ sensitivity strongest in the stratocumulus regime). While the spatial sensitivity patterns of the two satellite-derived aerosol proxies are well correlated, the $\log_{10}s$ sensitivities are not. CRE are much more sensitive to $\log_{10}$AI and $\log_{10}$AOD in the tropics, especially in the case of $\log_{10}$AOD, where the $\mathrm{CRE}_{LW}$ sensitivity is much higher than that of the other aerosol proxies and also higher than its $\mathrm{CRE}_{SW}$ sensitivity, which is likely caused by the statistical relationship between AOD, cloud fraction and cloud-top temperature in this region. It is assumed that the AI-CRE relationship is less strongly confounded by humidity than the AOD-CRE relationship, which cannot be fully controlled for as the relative humidity matters on much smaller scales. Differences between the sensitivities of CRE to $\log_{10}s$ and the satellite-derived aerosol proxies can additionally be explained be the varying contributions of $\log_{10}s$ to CCN globally.

The statistical framework suggested here and the derived sensitivity patterns can be used in future cloud feedback analyses and to compare relationships between CCFs and CRE in global climate model output.

*Data availability.* The ERA5 meteorological reanalysis data (https://doi.org/10.24381/cds.f17050d7; https://doi.org/10.24381/cds.6860a573) are freely available at the Copernicus Climate Change Service (C3S) Climate Date Store: https://cds.climate.copernicus.eu/#!/search?text=ERA5&type=dataset (last access: March 26th, 2021). MODIS data (https://dx.doi.org/10.5067/MODIS/MOD08_M3.061) were downloaded (last access: November 11th, 2021) in the Level-1 and Atmosphere Archive & Distribution System (LAADS) Distributed Active Archive Center (DAAC) https://ladsweb.modaps.eosdis.nasa.gov/search/. CERES data (https://doi.org/10.5067/TERRA-AQUA/CERES/EBAF-TOA_L3B004.1) are freely available and were obtained from the NASA Langley Research Center CERES ordering tool at https://ceres.larc.nasa.gov/ (last access: May 17th, 2021).

*Author contributions.* HA had the idea for the analysis, obtained and analyzed the data sets, and conducted the original research. HA wrote the article with contributions from all authors on the text and interpretation of the findings.

*Competing interests.* At least one of the (co-)authors is a member of the editorial board of Atmospheric Chemistry and Physics.

https://doi.org/10.5194/egusphere-2023-1283
Preprint. Discussion started: 14 June 2023


*Acknowledgements.* HA and JC have received funding from the European Union's Horizon 2020 research and innovation program under grant agreement no. 821205 (FORCeS) and the Deutsche Forschungsgemeinschaft (DFG) in the project Constraining Aerosol-Low cloud InteractionS with multi-target MAchine learning (CALISMA), project number 440521482. PS was supported by the European Research Council project RECAP under the European Union's Horizon 2020 research and innovation programme (grant no. 724602) and by the FORCeS project under the European Union's Horizon 2020 research programme with grant agreement no. 821205. PN and SWK were supported through the UK Natural Environment Research Council (NERC) grant number NE/V012045/1. CJW received funding from the European Union's Horizon 2020 research and innovation programme under the Marie Skłodowska-Curie grant agreement No 101019911. T.A.M. was supported by the NOAA Cooperative Agreements with CIRES, NA17OAR4320101 and NA22OAR4320151, and by the NOAA/ESRL Atmospheric Science for Renewable Energy program.

## References

Ackerman, A. S., Kirkpatrick, M. P., Stevens, D. E., and Toon, O. B.: The impact of humidity above stratiform clouds on indirect aerosol climate forcing, Nature, 432, 1014–1017, https://doi.org/10.1038/nature03137.1., 2004.

Albrecht, B. A.: Aerosols, cloud microphysics, and fractional cloudiness, Science, 245, 1227–1230, https://doi.org/10.1126/science.245.4923.1227, 1989.

Altaratz, O., Koren, I., Remer, L., and Hirsch, E.: Review: Cloud invigoration by aerosols—Coupling between microphysics and dynamics, Atmospheric Research, 140, 38–60, https://doi.org/10.1016/j.atmosres.2014.01.009, 2014.

Andersen, H. and Cermak, J.: How thermodynamic environments control stratocumulus microphysics and interactions with aerosols, Environmental Research Letters, 10, 24 004, https://doi.org/10.1088/1748-9326/10/2/024004, http://dx.doi.org/10.1088/1748-9326/10/2/024004, 2015.

Andersen, H., Cermak, J., Fuchs, J., and Schwarz, K.: Global observations of cloud-sensitive aerosol loadings in low-level marine clouds, Journal of Geophysical Research: Atmospheres, 121, 12 936–12 946, https://doi.org/10.1002/2016JD025614, http://doi.wiley.com/10.1002/2016JD025614, 2016.

Andersen, H., Cermak, J., Fuchs, J., Knutti, R., and Lohmann, U.: Understanding the drivers of marine liquid-water cloud occurrence and properties with global observations using neural networks, Atmospheric Chemistry and Physics, 17, 9535–9546, https://doi.org/10.5194/acp-17-9535-2017, 2017.

Andersen, H., Cermak, J., Fuchs, J., Knippertz, P., Gaetani, M., Quinting, J., Sippel, S., and Vogt, R.: Synoptic-scale controls of fog and low-cloud variability in the Namib Desert, Atmospheric Chemistry and Physics, 20, 3415–3438, https://doi.org/10.5194/acp-20-3415-2020, 2020.

Andersen, H., Cermak, J., Zipfel, L., and Myers, T. A.: Attribution of observed recent decrease in low clouds over the northeastern Pacific to cloud-controlling factors, Geophysical Research Letters, 49, 1–10, https://doi.org/10.1029/2021gl096498, 2022.

Bellouin, N., Quaas, J., Gryspeerdt, E., Kinne, S., Stier, P., Watson-Parris, D., Boucher, O., Carslaw, K. S., Christensen, M., Daniau, A. L., Dufresne, J. L., Feingold, G., Fiedler, S., Forster, P., Gettelman, A., Haywood, J. M., Lohmann, U., Malavelle, F., Mauritsen, T., McCoy, D. T., Myhre, G., Mülmenstädt, J., Neubauer, D., Possner, A., Rugenstein, M., Sato, Y., Schulz, M., Schwartz, S. E., Sourdeval, O., Storelvmo, T., Toll, V., Winker, D., and Stevens, B.: Bounding Global Aerosol Radiative Forcing of Climate Change, Reviews of Geophysics, 58, 1–45, https://doi.org/10.1029/2019RG000660, 2020.

Bony, S. and Dufresne, J. L.: Marine boundary layer clouds at the heart of tropical cloud feedback uncertainties in climate models, Geophysical Research Letters, 32, 1–4, https://doi.org/10.1029/2005GL023851, 2005.

Ceppi, P. and Nowack, P.: Observational evidence that cloud feedback amplifies global warming, Proceedings of the National Academy of Sciences, 118, https://doi.org/10.1073/pnas.2026290118, https://www.pnas.org/content/118/30/e2026290118, 2021.

Cesana, G., Del Genio, D. A., Ackerman, S. A., Kelley, M., Elsaesser, G., Fridlind, M. A., Cheng, Y., and Yao, M. S.: Evaluating models response of tropical low clouds to SST forcings using CALIPSO observations, Atmospheric Chemistry and Physics, 19, 2813–2832, https://doi.org/10.5194/acp-19-2813-2019, 2019.

Cesana, G. V. and Del Genio, A. D.: Observational constraint on cloud feebacks suggests moderate climate sensitivity, Nature Climate Change, 11, 213–220, https://doi.org/10.1038/s41558-020-00970-y, http://dx.doi.org/10.1038/s41558-020-00970-y, 2021.

Chen, J., Liu, Y., Zhang, M., and Peng, Y.: New understanding and quantification of the regime dependence of aerosol-cloud interaction for studying aerosol indirect effects, Geophysical Research Letters, 43, 1780–1787, https://doi.org/10.1002/2016GL067683, 2016.

Chen, J., Liu, Y., Zhang, M., and Peng, Y.: Height Dependency of Aerosol-Cloud Interaction Regimes, Journal of Geophysical Research: Atmospheres, 123, 491–506, https://doi.org/10.1002/2017JD027431, 2018.

Chen, Y., Haywood, J., Wang, Y., Malavelle, F., Jordan, G., Partridge, D., Fieldsend, J., Leeuw, J. D., Schmidt, A., Cho, N., Oreopoulos, L., Platnick, S., Grosvenor, D., Field, P., and Lohmann, U.: Machine learning reveals climate forcing from aerosols is dominated by increased cloud cover, Nature Geoscience2, 15, 609–614, https://doi.org/10.1038/s41561-022-00991-6, 2022.

Christensen, M. W., Jones, W. K., and Stier, P.: Aerosols enhance cloud lifetime and brightness along the stratus-to-cumulus transition, Proceedings of the National Academy of Sciences of the United States of America, 117, 17 591–17 598, https://doi.org/10.1073/pnas.1921231117, 2020.

Christensen, W. M., Neubauer, D., Poulsen, A. C., Thomas, E. G., McGarragh, R. G., Povey, C. A., Proud, R. S., and Grainger, G. R.: Unveiling aerosol-cloud interactions - Part 1: Cloud contamination in satellite products enhances the aerosol indirect forcing estimate, Atmospheric Chemistry and Physics, 17, 13 151–13 164, https://doi.org/10.5194/acp-17-13151-2017, 2017.

de Szoeke, S. P., Verlinden, K. L., Yuter, S. E., and Mechem, D. B.: The time scales of variability of marine low clouds, Journal of Climate, 29, 6463–6481, https://doi.org/10.1175/JCLI-D-15-0460.1, 2016.

Eytan, E., Koren, I., Altaratz, O., Kostinski, A. B., and Ronen, A.: Longwave radiative effect of the cloud twilight zone, Nature Geoscience, https://doi.org/10.1038/s41561-020-0636-8, http://dx.doi.org/10.1038/s41561-020-0636-8, 2020.

Forster, P., Storelvmo, T., Armour, K., Collins, W., Dufresne, J.-L., Frame, D., Lunt, D. J., Mauritsen, T., Palmer, M. D., Watanabe, M., Wild, M., and Zhang, H.: The Earth's Energy Budget, Climate Feedbacks, and Climate Sensitivity, https://doi.org/10.1017/9781009157896.009, 2021.

Fuchs, J., Cermak, J., Andersen, H., Hollmann, R., and Schwarz, K.: On the Influence of Air Mass Origin on Low-Cloud Properties in the Southeast Atlantic, Journal of Geophysical Research: Atmospheres, 122, 11,076–11,091, https://doi.org/10.1002/2017JD027184, 2017.

Fuchs, J., Cermak, J., and Andersen, H.: Building a cloud in the Southeast Atlantic: Understanding low-cloud controls based on satellite observations with machine learning, Atmospheric Chemistry and Physics, 18, 16 537–16 552, https://doi.org/10.5194/acp-2018-593, 2018.

Fueglistaler, S.: Observational Evidence for Two Modes of Coupling Between Sea Surface Temperatures, Tropospheric Temperature Profile, and Shortwave Cloud Radiative Effect in the Tropics, Geophysical Research Letters, 46, 9890–9898, https://doi.org/10.1029/2019GL083990, 2019.

Ge, J., Wang, Z., Wang, C., Yang, X., Dong, Z., and Wang, M.: Diurnal variations of global clouds observed from the CATS spaceborne lidar and their links to large - scale meteorological factors, Climate Dynamics, 57, 2637–2651, https://doi.org/10.1007/s00382-021-05829-2, https://doi.org/10.1007/s00382-021-05829-2, 2021.

Gjermundsen, A., Nummelin, A., Olivié, D., Bentsen, M., Seland, Ø., and Schulz, M.: Shutdown of Southern Ocean convection controls long-term greenhouse gas-induced warming, Nature Geoscience, 14, 724–731, https://doi.org/10.1038/s41561-021-00825-x, http://dx.doi.org/10.1038/s41561-021-00825-x, 2021.

Grandey, B. S. and Stier, P.: A critical look at spatial scale choices in satellite-based aerosol indirect effect studies, Atmospheric Chemistry and Physics, 10, 11 459–11 470, https://doi.org/10.5194/acp-10-11459-2010, http://www.atmos-chem-phys.net/10/11459/2010/, 2010.

Grandey, B. S., Stier, P., and Wagner, T. M.: Investigating relationships between aerosol optical depth and cloud fraction using satellite, aerosol reanalysis and general circulation model data, Atmospheric Chemistry and Physics, 13, 3177–3184, https://doi.org/10.5194/acp-13-3177-2013, 2013.

Grise, K. M. and Kelleher, M. K.: Midlatitude cloud radiative effect sensitivity to cloud controlling factors in observations and models: Relationship with southern hemisphere jet shifts and climate sensitivity, Journal of Climate, 34, 5869–5886, https://doi.org/10.1175/JCLI-D-20-0986.1, 2021.

Gryspeerdt, E., Stier, P., and Grandey, B. S.: Cloud fraction mediates the aerosol optical depth-cloud top height relationship, Geophysical Research Letters, 41, 3622–3627, https://doi.org/10.1002/2014GL059524, 2014.

Gryspeerdt, E., Quaas, J., and Bellouin, N.: Constraining the aerosol influence on cloud fraction, Journal of Geophysical Research: Atmospheres, 121, 3566–3583, https://doi.org/10.1002/2015JD023744, 2016.

Gryspeerdt, E., Sourdeval, O., Quaas, J., Delanoë, J., Krämer, M., and Kühne, P.: Ice crystal number concentration estimates from lidar-radar satellite remote sensing - Part 2: Controls on the ice crystal number concentration, Atmospheric Chemistry and Physics, 18, 14 351–14 370, https://doi.org/10.5194/acp-18-14351-2018, 2018.

Gryspeerdt, E., Smith, T. W. P., O'Keeffe, E., Christensen, M. W., and Goldsworth, F. W.: The Impact of Ship Emission Controls Recorded by Cloud Properties, Geophysical Research Letters, 46, 2019GL084 700, https://doi.org/10.1029/2019GL084700, https://onlinelibrary.wiley.com/doi/abs/10.1029/2019GL084700, 2019.

Hasekamp, O. P., Gryspeerdt, E., and Quaas, J.: Analysis of polarimetric satellite measurements suggests stronger cooling due to aerosol-cloud interactions, Nature Communications, 2, 1–7, https://doi.org/10.1038/s41467-019-13372-2, http://dx.doi.org/10.1038/s41467-019-13372-2, 2019.

Hastie, T., Tibshirani, R., and Friedman, J.: The Elements of Statistical Learning, Springer Series in Statistics New York, NY, USA, 2nd edn., 2001.

Hastie, T., Tibshirani, R., James, G., and Witten, D.: An introduction to statistical learning (2nd ed.), Springer texts, 102, 618, 2021.

Hersbach, H., Bell, B., Berrisford, P., Biavati, G., Horányi, A., Muñoz Sabater, J., Nicolas, J., Peubey, C., Radu, R., Rozum, I., Schepers, D., Simmons, A., Soci, C., Dee, D., and Thépaut, J.-N.: ERA5 monthly averaged data on pressure levels from 1979 to present. Copernicus Climate Change Service (C3S) Climate Data Store (CDS). (Last accessed on 12-05-2021), https://doi.org/10.24381/cds.6860a573, 2019a.

Hersbach, H., Bell, B., Berrisford, P., Biavati, G., Horányi, A., Muñoz Sabater, J., Nicolas, J., Peubey, C., Radu, R., Rozum, I., Schepers, D., Simmons, A., Soci, C., Dee, D., and Thépaut, J.-N.: ERA5 monthly averaged data on single levels from 1979 to present. Copernicus Climate Change Service (C3S) Climate Data Store (CDS). (Last accessed on 12-05-2021), https://doi.org/10.24381/cds.f17050d7, 2019b.

Hoose, C. and Möhler, O.: Heterogeneous ice nucleation on atmospheric aerosols: A review of results from laboratory experiments, vol. 12, https://doi.org/10.5194/acp-12-9817-2012, 2012.

Jahani, B., Andersen, H., Calbó, J., González, J.-A., and Cermak, J.: Longwave Radiative Effect of the Cloud-Aerosol Transition Zone Based on CERES Observations, Atmospheric Chemistry and Physics, pp. 1–17, https://doi.org/10.5194/acp-2021-421, 2021.

Jia, H., Ma, X., Yu, F., and Quaas, J.: Significant underestimation of radiative forcing by aerosol–cloud interactions derived from satellite-based methods, Nature Communications, 12, 1–12, https://doi.org/10.1038/s41467-021-23888-1, http://dx.doi.org/10.1038/s41467-021-23888-1, 2021.

Kärcher, B.: Formation and radiative forcing of contrail cirrus, Nature Communications, 9, 1–17, https://doi.org/10.1038/s41467-018-04068-0, http://dx.doi.org/10.1038/s41467-018-04068-0, 2018.

Kaufman, Y. J. and Koren, I.: Smoke and Pollution Aerosol Effect on Cloud Cover, Science, 313, 655–658, https://doi.org/10.1126/science.1126232, 2006.

Kelleher, M. K. and Grise, K. M.: Examining Southern Ocean cloud controlling factors on daily time scales and their connections to midlatitude weather systems, Journal of Climate, 32, 5145–5160, https://doi.org/10.1175/JCLI-D-18-0840.1, 2019.

https://doi.org/10.5194/egusphere-2023-1283
Preprint. Discussion started: 14 June 2023


Klein, S. A. and Hartmann, D. L.: The Seasonal Cycle of Low Stratiform Clouds, Journal of Climate, 6, 1587–1606, https://doi.org/10.1175/1520-0442(1993)006<1587:TSCOLS>2.0.CO;2, 1993.

Klein, S. A., Hartmann, D. L., and Norris, J. R.: On the Relationships among Low-Cloud Structure, Sea Surface Temperature, and Atmospheric Circulation in the Summertime Northeast Pacific, Journal of Climate, 8, 1140–1155, https://doi.org/10.1175/1520-0442(1995)008<1140:OTRALC>2.0.CO;2, 1995.

Klein, S. A., Hall, A., Norris, J. R., and Pincus, R.: Low-Cloud Feedbacks from Cloud-Controlling Factors: A Review, Surveys in Geophysics, 38, 1307–1329, https://doi.org/10.1007/s10712-017-9433-3, 2017.

Kopec, M. K., Malinowski, S. P., and Piotrowski, Z. P.: Effects of wind shear and radiative cooling on the stratocumulus-topped boundary layer, Quarterly Journal of the Royal Meteorological Society, 142, 3222–3233, https://doi.org/10.1002/qj.2903, 2016.

Koren, I., Kaufman, Y. J., Rosenfeld, D., Remer, L. A., and Rudich, Y.: Aerosol invigoration and restructuring of Atlantic convective clouds, Geophysical Research Letters, 32, L14 828, https://doi.org/10.1029/2005GL023187, http://doi.wiley.com/10.1029/2005GL023187, 2005.

Koren, I., Feingold, G., and Remer, L. A.: The invigoration of deep convective clouds over the Atlantic: Aerosol effect, meteorology or retrieval artifact?, Atmospheric Chemistry and Physics, 10, 8855–8872, https://doi.org/10.5194/acp-10-8855-2010, 2010.

Koren, I., Dagan, G., and Altaratz, O.: From aerosol-limited to invigoration of warm convective clouds, Science, 344, 1143–1146, https://doi.org/10.1126/science.1252595, http://www.sciencemag.org/content/344/6188/1143.full, 2014.

Loeb, N. G., Doelling, D. R., Wang, H., Su, W., Nguyen, C., Corbett, J. G., Liang, L., Mitrescu, C., Rose, F. G., and Kato, S.: Clouds and the Earth'S Radiant Energy System (CERES) Energy Balanced and Filled (EBAF) top-of-atmosphere (TOA) edition-4.0 data product, Journal of Climate, 31, 895–918, https://doi.org/10.1175/JCLI-D-17-0208.1, 2018.

Malavelle, F. F., Haywood, J. M., Jones, A., Gettelman, A., Clarisse, L., Bauduin, S., Allan, R. P., Karset, I. H. H., Kristjánsson, J. E., Oreopoulos, L., Cho, N., Lee, D., Bellouin, N., Boucher, O., Grosvenor, D. P., Carslaw, K. S., Dhomse, S., Mann, G. W., Schmidt, A., Coe, H., Hartley, M. E., Dalvi, M., Hill, A. A., Johnson, B. T., Johnson, C. E., Knight, J. R., O'Connor, F. M., Stier, P., Myhre, G., Platnick, S., Stephens, G. L., Takahashi, H., and Thordarson, T.: Strong constraints on aerosol-cloud interactions from volcanic eruptions, Nature, 546, 485–491, https://doi.org/10.1038/nature22974, http://dx.doi.org/10.1038/nature22974, 2017.

Mallet, M. D., Protat, A., Alexander, S. P., and Fiddes, S. L.: Reducing Southern Ocean shortwave radiation errors in the ERA5 reanalysis with machine learning and 25 years of surface observations, Artificial Intelligence for the Earth Systems, In prep, 1–42, https://doi.org/10.1175/AIES-D-22-0044, 2022.

Manshausen, P., Watson-parris, D., Christensen, M. W., Jalkanen, J.-p., and Stier, P.: Invisible ship tracks show large cloud sensitivity to aerosol, Nature, 610, 101–106, https://doi.org/10.1038/s41586-022-05122-0, 2022.

Marinescu, P. J., Van Den Heever, S. C., Heikenfeld, M., Barrett, A. I., Barthlott, C., Hoose, C., Fan, J., Fridlind, A. M., Matsui, T., Miltenberger, A. K., Stier, P., Vie, B., White, B. A., and Zhang, Y.: Impacts of varying concentrations of cloud condensation nuclei on deep convective cloud updrafts a multimodel assessment, Journal of the Atmospheric Sciences, 78, 1147–1172, https://doi.org/10.1175/JAS-D-20-0200.1, 2021.

Mauger, G. S. and Norris, J. R.: Assessing the impact of meteorological history on subtropical cloud fraction, Journal of Climate, 23, 2926–2940, https://doi.org/10.1175/2010JCLI3272.1, 2010.

McCoy, D. T., Eastman, R., Hartmann, D. L., and Wood, R.: The change in low cloud cover in a warmed climate inferred from AIRS, MODIS, and ERA-interim, Journal of Climate, 30, 3609–3620, https://doi.org/10.1175/JCLI-D-15-0734.1, 2017.

https://doi.org/10.5194/egusphere-2023-1283
Preprint. Discussion started: 14 June 2023


McCoy, D. T., Bender, F. A., Grosvenor, D. P., Mohrmann, J. K., Hartmann, D. L., Wood, R., and Field, P. R.: Predicting decadal trends in cloud droplet number concentration using reanalysis and satellite data, Atmospheric Chemistry and Physics, 18, 2035–2047, https://doi.org/10.5194/acp-18-2035-2018, 2018.

McFarquhar, G. M., Bretherton, C. S., Marchand, R., Protat, A., DeMott, P. J., Alexander, S. P., Roberts, G. C., Twohy, C. H., Toohey, D., Siems, S., Huang, Y., Wood, R., Rauber, R. M., Lasher-Trapp, S., Jensen, J., Stith, J. L., Mace, J., Um, J., Järvinen, E., Schnaiter, M., Gettelman, A., Sanchez, K. J., McCluskey, C. S., Russell, L. M., McCoy, I. L., Atlas, R. L., Bardeen, C. G., Moore, K. A., Hill, T. C., Humphries, R. S., Keywood, M. D., Ristovski, Z., Cravigan, L., Schofield, R., Fairall, C., Mallet, M. D., Kreidenweis, S. M., Rainwater, B., D'Alessandro, J., Wang, Y., Wu, W., Saliba, G., Levin, E. J., Ding, S., Lang, F., Truong, S. C., Wolff, C., Haggerty, J., Harvey, M. J., Klekociuk, A. R., and McDonald, A.: Observations of clouds, aerosols, precipitation, and surface radiation over the southern ocean, Bulletin of the American Meteorological Society, 102, E894–E928, https://doi.org/10.1175/BAMS-D-20-0132.1, 2021.

Medeiros, B. and Stevens, B.: Revealing differences in GCM representations of low clouds, Climate Dynamics, 36, 385–399, https://doi.org/10.1007/s00382-009-0694-5, 2011.

Mülmenstädt, J., Salzmann, M., Kay, J. E., Zelinka, M. D., Ma, P.-L., Nam, C., Kretzschmar, J., Hörnig, S., and Quaas, J.: An underestimated negative cloud feedback from cloud lifetime changes, Nature Climate Change, 11, 508–513, https://doi.org/10.1038/s41558-021-01038-1, http://dx.doi.org/10.1038/s41558-021-01038-1, 2021.

Murray, B. J., Carslaw, K. S., and Field, P. R.: Opinion: Cloud-phase climate feedback and the importance of ice-nucleating particles, Atmospheric Chemistry and Physics, 21, 665–679, https://doi.org/10.5194/acp-21-665-2021, 2021.

Murray-Watson, R. J. and Gryspeerdt, E.: Stability dependent increases in liquid water with droplet number in the Arctic, Atmospheric Chemistry and Physics Discussions, pp. 1–17, https://doi.org/10.5194/acp-2021-861, 2021.

Myers, T. A. and Norris, J. R.: Observational evidence that enhanced subsidence reduces subtropical marine boundary layer cloudiness, Journal of Climate, 26, 7507–7524, https://doi.org/10.1175/JCLI-D-12-00736.1, 2013.

Myers, T. A. and Norris, J. R.: Reducing the uncertainty in subtropical cloud feedback, Geophysical Research Letters, 43, 2144–2148, https://doi.org/10.1002/2015GL067416, 2016.

Myers, T. A., Mechoso, C. R., and DeFlorio, M. J.: Coupling between marine boundary layer clouds and summer-to-summer sea surface temperature variability over the North Atlantic and Pacific, Climate Dynamics, 50, 955–969, https://doi.org/10.1007/s00382-017-3651-8, 2018.

Myers, T. A., Scott, R. C., Zelinka, M. D., Klein, S. A., Norris, J. R., and Caldwell, P. M.: Observational constraints on low cloud feedback reduce uncertainty of climate sensitivity, Nature Climate Change, https://doi.org/10.1038/s41558-021-01039-0, http://dx.doi.org/10.1038/s41558-021-01039-0, 2021.

Nakajima, T., Higurashi, A., Kawamoto, K., and Penner, J. E.: A possible correlation between satellite-derived cloud and aerosol microphysical parameters, Geophysical Research Letters, 28, 1171–1174, https://doi.org/10.1029/2000GL012186, 2001.

Patil, P., Wei, Y. W., Rinaldo, A., and Tibshirani, R. J.: Uniform consistency of cross-validation estimators for high-dimensional ridge regression, International Conference on Artificial Intelligence and Statistics, 1, 1–10, 2021.

Patnaude, R., Diao, M., Liu, X., and Chu, S.: Effects of thermodynamics, dynamics and aerosols on cirrus clouds based on in situ observations and NCAR CAM6, Atmospheric Chemistry and Physics, 21, 1835–1859, https://doi.org/10.5194/acp-21-1835-2021, 2021.

Qu, X., Hall, A., Klein, S. A., and Deangelis, A. M.: Positive tropical marine low-cloud cover feedback inferred from cloud-controlling factors, Geophysical Research Letters, 42, 7767–7775, https://doi.org/10.1002/2015GL065627, 2015.

https://doi.org/10.5194/egusphere-2023-1283
Preprint. Discussion started: 14 June 2023


Quaas, J., Jia, H., Smith, C., Albright, A. L., Aas, W., Bellouin, N., Boucher, O., Doutriaux-Boucher, M., Forster, P. M., Grosvenor, D., Jenkins, S., Klimont, Z., Loeb, N. G., Ma, X., Naik, V., Paulot, F., Stier, P., Wild, M., Myhre, G., and Schulz, M.: Robust evidence for reversal of the trend in aerosol effective climate forcing, Atmospheric Chemistry and Physics, 22, 12 221–12 239, https://doi.org/10.5194/acp-22-12221-2022, 2022.

Ramanathan, V., Cess, R. D., Harrison, E. F., Minnis, P., Barkstrom, B. R., Ahmad, E., and Hartmann, D.: Cloud-Radiative Forcing and Climate: Results from the Earth Radiation Budget Experiment, Science, 243, 57–63, https://doi.org/10.1126/science.243.4887.57, 1989.

Randles, C. A., da Silva, A. M., Buchard, V., Colarco, P. R., Darmenov, A., Govindaraju, R., Smirnov, A., Holben, B., Ferrare, R., Hair, J., Shinozuka, Y., and Flynn, C. J.: The MERRA-2 aerosol reanalysis, 1980 onward. Part I: System description and data assimilation evaluation, Journal of Climate, 30, 6823–6850, https://doi.org/10.1175/JCLI-D-16-0609.1, 2017.

Rieck, M., Nuijens, L., and Stevens, B.: Marine boundary layer cloud feedbacks in a constant relative humidity atmosphere, Journal of the Atmospheric Sciences, 69, 2538–2550, https://doi.org/10.1175/JAS-D-11-0203.1, 2012.

Rosenfeld, D., Zhu, Y., Wang, M., Zheng, Y., Goren, T., and Yu, S.: Aerosol-driven droplet concentrations dominate coverage and water of oceanic low-level clouds, Science, 363, https://doi.org/10.1126/science.aav0566, 2019.

Sarangi, C., Kanawade, V. P., Tripathi, S. N., Thomas, A., and Ganguly, D.: Aerosol-induced intensification of cooling effect of clouds during Indian summer monsoon, Nature Communications, 9, https://doi.org/10.1038/s41467-018-06015-5, http://dx.doi.org/10.1038/s41467-018-06015-5, 2018.

Schwarz, K., Cermak, J., Fuchs, J., and Andersen, H.: Mapping the Twilight Zone—What We Are Missing between Clouds and Aerosols, Remote Sensing, 9, 577, https://doi.org/10.3390/rs9060577, http://www.mdpi.com/2072-4292/9/6/577, 2017.

Scott, R. C., Myers, T. A., Norris, J. R., Zelinka, M. D., Klein, S. A., Sun, M., and Doelling, D. R.: Observed sensitivity of low-cloud radiative effects to meteorological perturbations over the global oceans, Journal of Climate, 33, 7717–7734, https://doi.org/10.1175/JCLI-D-19-1028.1, 2020.

Stevens, B. and Feingold, G.: Untangling aerosol effects on clouds and precipitation in a buffered system, Nature, 461, 607–613, https://doi.org/10.1038/nature08281, http://www.ncbi.nlm.nih.gov/pubmed/19794487, 2009.

Stier, P.: Limitations of passive remote sensing to constrain global cloud condensation nuclei, Atmospheric Chemistry and Physics, 16, 6595–6607, https://doi.org/10.5194/acp-16-6595-2016, http://www.atmos-chem-phys.net/16/6595/2016/, 2016.

Toll, V., Christensen, M., Quaas, J., and Bellouin, N.: Weak average liquid-cloud-water response to anthropogenic aerosols, Nature, 572, 51–55, https://doi.org/10.1038/s41586-019-1423-9, http://dx.doi.org/10.1038/s41586-019-1423-9, 2019.

Twomey, S.: The Influence of Pollution on the Shortwave Albedo of Clouds, Journal of the Atmospheric Sciences, 34, 1149–1152, https://doi.org/10.1175/1520-0469(1977)034<1149:TIOPOT>2.0.CO;2, 1977.

van der Dussen, J. J., de Roode, S. R., Dal Gesso, S., and Siebesma, A. P.: An LES model study of the influence of the free tropospheric thermodynamic conditions on the stratocumulus response to a climate perturbation, Journal of Advances in Modeling Earth Systems, 7, 670–691, https://doi.org/10.1002/2014MS000380, 2015.

Vergara-Temprado, J., Miltenberger, A. K., Furtado, K., Grosvenor, D. P., Shipway, B. J., Hill, A. A., Wilkinson, J. M., Field, P. R., Murray, B. J., and Carslaw, K. S.: Strong control of Southern Ocean cloud reflectivity by ice-nucleating particles, Proceedings of the National Academy of Sciences of the United States of America, 115, 2687–2692, https://doi.org/10.1073/pnas.1721627115, 2018.

Voigt, A., Albern, N., Ceppi, P., Grise, K., Li, Y., and Medeiros, B.: Clouds, radiation, and atmospheric circulation in the present-day climate and under climate change, Wiley Interdisciplinary Reviews: Climate Change, 12, 1–22, https://doi.org/10.1002/wcc.694, 2021.

https://doi.org/10.5194/egusphere-2023-1283
Preprint. Discussion started: 14 June 2023


Wall, C. J., Hartmann, D. L., and Norris, J. R.: Is the Net Cloud Radiative Effect Constrained to be Uniform Over the Tropical Warm Pools?, Geophysical Research Letters, 46, 12 495–12 503, https://doi.org/10.1029/2019GL083642, 2019.

Wall, C. J., Norris, J. R., Possner, A., McCoy, D. T., McCoy, I. L., and Lutsko, N. J.: Assessing effective radiative forcing from aerosol-cloud interactions over the global ocean, Proceedings of the National Academy of Sciences of the United States of America, 119, https://doi.org/10.1073/pnas.2210481119, 2022.

Wood, R.: Stratocumulus Clouds, Monthly Weather Review, 140, 2373–2423, https://doi.org/10.1175/MWR-D-11-00121.1, 2012.

Wood, R. and Bretherton, C. S.: On the relationship between stratiform low cloud cover and lower-tropospheric stability, Journal of Climate, 19, 6425–6432, https://doi.org/10.1175/JCLI3988.1, 2006.

Zamora Zapata, M., Heus, T., and Kleissl, J.: Effects of Surface and Top Wind Shear on the Spatial Organization of Marine Stratocumulus-Topped Boundary Layers, Journal of Geophysical Research: Atmospheres, 126, 1–18, https://doi.org/10.1029/2020JD034162, 2021.

Zelinka, M. D., Zhou, C., and Klein, S. A.: Insights from a refined decomposition of cloud feedbacks, Geophysical Research Letters, 43, 9259–9269, https://doi.org/10.1002/2016GL069917, 2016.

Zelinka, M. D., Myers, T. A., McCoy, D. T., Po-Chedley, S., Caldwell, P. M., Ceppi, P., Klein, S. A., and Taylor, K. E.: Causes of Higher Climate Sensitivity in CMIP6 Models, Geophysical Research Letters, 47, e2019GL085 782, https://doi.org/10.1029/2019GL085782, 2020.

Zelinka, M. D., Tan, I., Oreopoulos, L., and Tselioudis, G.: Detailing cloud property feedbacks with a regime - based decomposition, Climate Dynamics, https://doi.org/10.1007/s00382-022-06488-7, https://doi.org/10.1007/s00382-022-06488-7, 2022.

Zhang, C.: Large-Scale Variability of Atmospheric Deep Convection in Relation to Sea Surface Temperature in the Tropics, Journal of Climate, 6, 1898–1913, https://doi.org/10.1175/1520-0442(1993)006<1898:LSVOAD>2.0.CO;2, http://journal.um-surabaya.ac.id/index.php/JKM/article/view/2203, 1993.

Zipfel, L., Andersen, H., and Cermak, J.: Machine-Learning Based Analysis of Liquid Water Path Adjustments to Aerosol Perturbations in Marine Boundary Layer Clouds Using Satellite Observations, Atmosphere, 13, 586, https://doi.org/10.3390/atmos13040586, 2022.

Zuidema, P., Painemal, D., de Szoeke, S., and Fairall, C.: Stratocumulus Cloud-Top Height Estimates and Their Climatic Implications, Journal of Climate, 22, 4652–4666, https://doi.org/10.1175/2009JCLI2708.1, 2009.